UCLA
COMPUTATIONAL AND APPLIED MATHEMATICS

A General Technique for Eliminating Spurious Oscillations in Conservative Schemes for Multiphase and Multispecies Euler Equations

Ronald P. Fedkiw
Xu-Dong Liu
Stanley Osher

June 1997

CAM Report 97-27

Department of Mathematics
University of California, Los Angeles
Los Angeles, CA. 90095-1555

A General Technique for Eliminating Spurious Oscillations in Conservative Schemes for Multiphase and Multispecies Euler Equations

Ronald P. Fedkiw
Xu-Dong Liu
Stanley Osher *

June 10, 1997

Abstract

Standard conservative schemes have been shown to admit nonphysical oscillations near some material interfaces. For example, the calorically perfect Euler equations have been shown to admit these oscillations when there is a jump in both temperature and gamma across an interface, but not when either temperature or gamma is constant [4].

For most problems, one can obtain adequate numerical results by applying a fully conservative method to the mass fraction formulation of the problem. Comparable results can also be obtained with the level set formulation of the problem, as long as gamma is reconstructed in a smooth way from the level set function. Occasionally, the conservative method will admit nonphysical oscillations which can be avoided by application of a nonconservative correction to the total energy on a set of measure zero under grid refinement. We outline this correction method, drawing heavily on the work in [5].

*Research supported in part by ONR N00014-97-1-0027, ARPA URI-ONR-N00014-92-J-1890, NSF #DMS 94-04942, and ARO DAAH04-95-1-0155

1 Introduction

Standard conservative schemes have been shown to admit nonphysical oscillations near material interfaces, e.g. see Karni [5]. Jenny, Muller, and Thomann [4] specifically consider the calorically perfect Euler equations and show that these nonphysical oscillations are inherent to standard conservative schemes when there is a jump in both temperature and gamma across an interface, but do not occur when either temperature or gamma is constant. Both [5] and [4] propose schemes which modify the conservative formulation of the equations in regions where difficulties may occur. These modifications give rise to conservation errors in the total energy of the system, and thus yield a locally nonconservative formulation.

In general, nonconservative formulations give the wrong shock speeds, although the errors in shock speeds can be reduced significantly if a special viscosity term is added [6]. Neither [5] nor [4] make use of this special viscosity term. Their schemes are fully conservative, except on a set of measure zero under grid refinement, and seem to give adequate shock speeds for numerical purposes on real problems, see e.g. [8].

In [5], the examples seem to indicate that the mass fraction formulation is nearly adequate in the fully conservative framework, while the level set formulation (used carelessly) admits wild nonphysical oscillations on the same problems. The cause of these oscillations for level set methods stems back to [7], where the authors used the level set formulation in order to reconstruct gamma as a Heaviside function (jump discontinuity), even though the density was numerically smeared out. Sussman et. al. [9] solved a similar problem where he found that construction of a Heaviside density function from the level set function was inadequate for numerical purposes, and instead imposed an artificial smearing of the density near the interface in order to numerically well condition the problem. When this idea is applied to the work in [5], one can easily see that a smeared out version of gamma will behave better than a Heaviside function. In fact, the smoothing of gamma could be chosen to approximate the numerical dissipation encountered when solving the mass fraction equation. Thus, proper reconstruction of gamma from the level set formulation will eliminate all of the large oscillations shown in [5], leaving only small problems similar to those shown in the mass fraction formulations. It should be noted that the level set function is not essential

in two phase problems where the interface can be captured (e.g. many compressible flow problems) and a mass fraction formulation could be used, as opposed to some incompressible two phase problems (e.g. [9]) where the level set function is essential.

It would appear that the conservative formulation is almost good enough and that there is no real need to use these nonconservative corrections. In fact, we believe that this is the case for most problems. However, the mass fraction formulation examples in [5] are misleading, since they only show minor numerical difficulty, while examples do exist with large oscillations.

In summary, the conservative formulation of the problem will usually give a solution with little to no difficulties for the mass fraction formulation and the level set formulation, as long as gamma is reconstructed in a smooth way. However, there will be occasions where both formulations admit large nonphysical oscillations, and here a nonconservative correction method will be applied locally. Thus, we follow along the lines of [4] by formulating the problem in a conservative fashion and only applying the nonconservative method as a local correction to an existing conservative solver. Our nonconservative correction method is based on the approach in [5].

It should be noted that the authors in [4] only consider the case of the calorically perfect Euler equations, when they show that simultaneous jumps in both temperature and gamma are the cause of the oscillations. In fact, we will present one case where large jumps in both temperature and gamma admit no oscillations, and another case where much smaller jumps admit wild oscillations (using the *thermally* perfect Euler equations). In general, the cause of nonphysical oscillations at an interface will depend on the formulation of the problem and could be dependent on many factors, e.g. mass fractions, the level set function, gamma, temperature, and equations of state.

2 Euler Equations

Consider the two dimensional thermally perfect Euler Equations for multi-species flow with a total of N species,

$$\vec{U}_t + [\vec{F}(\vec{U})]_x + [\vec{G}(\vec{U})]_y = 0, \tag{1}$$

$$\vec{U} = \begin{pmatrix} \rho \\ \rho u \\ \rho v \\ E \\ \rho Y_1 \\ \vdots \\ \rho Y_{N-1} \end{pmatrix}, \quad \vec{F}(\vec{U}) = \begin{pmatrix} \rho u \\ \rho u^2 + p \\ \rho uv \\ (E+p)u \\ \rho u Y_1 \\ \vdots \\ \rho u Y_{N-1} \end{pmatrix}, \quad \vec{G}(\vec{U}) = \begin{pmatrix} \rho v \\ \rho uv \\ \rho v^2 + p \\ (E+p)v \\ \rho v Y_1 \\ \vdots \\ \rho v Y_{N-1}, \end{pmatrix} \tag{2}$$

$$E = -p + \frac{\rho(u^2+v^2)}{2} + \rho\left(\sum_{i=1}^{N} Y_i h_i\right), \qquad h_i(T) = h_i^f + \int_0^T c_{p,i}(s)ds \tag{3}$$

where t is time, x and y are the spatial dimensions, ρ is the density, u and v are the velocities, E is the energy per unit volume, Y_i is the mass fraction of species i, h_i is the enthalpy per unit mass of species i, h_i^f is the heat of formation of species i (enthalpy at $0K$), $c_{p,i}$ is the specific heat at constant pressure of species i, and p is the pressure [2]. Note that $Y_N = 1 - \sum_{i=1}^{N-1} Y_i$.

The pressure is a function of the density, internal energy per unit mass, and the mass fractions, $p = p(\rho, e, Y_1, \cdots, Y_{N-1})$, and the corresponding partial derivatives are denoted by p_ρ, p_e and p_{Y_i}. Note that $E = \rho e + \frac{\rho(u^2+v^2)}{2}$, expresses the the internal energy per unit mass in relation to the other variables.

The eigenvalues and eigenvectors for the Jacobian matrix of $\vec{F}(\vec{U})$, are obtained by setting $A = 1$ and $B = 0$ in the following formulas, while those for the Jacobian matrix of $\vec{G}(\vec{U})$ use $A = 0$ and $B = 1$.

The eigenvalues are

$$\lambda^1 = \hat{u} - c, \quad \lambda^{N+3} = \hat{u} + c \tag{4}$$

$$\lambda^2 = \cdots = \lambda^{N+2} = \hat{u}. \tag{5}$$

Note the $(N+1)$-fold repeated eigenvalue. We will make use of this and apply the Complementary Projection Method (CPM) for eigensystem treatment [1]. In the CPM method, full upwinding is accomplished without use of the eigenvectors in the repeated eigenvalue field. Thus, the necessary left and right eigenvectors are:

$$\vec{L}^1 = \left(\frac{b_2}{2} + \frac{\hat{u}}{2c} + \frac{b_3}{2}, -\frac{b_1 u}{2} - \frac{A}{2c}, -\frac{b_1 v}{2} - \frac{B}{2c}, \frac{b_1}{2}, \frac{-b_1 z_1}{2}, \cdots, \frac{-b_1 z_{N-1}}{2}\right) \quad (6)$$

$$\vec{L}^{N+3} = \left(\frac{b_2}{2} - \frac{\hat{u}}{2c} + \frac{b_3}{2}, -\frac{b_1 u}{2} + \frac{A}{2c}, -\frac{b_1 v}{2} + \frac{B}{2c}, \frac{b_1}{2}, \frac{-b_1 z_1}{2}, \cdots, \frac{-b_1 z_{N-1}}{2}\right) \quad (7)$$

$$\vec{R}^1 = \begin{pmatrix} 1 \\ u - Ac \\ v - Bc \\ H - \hat{u}c \\ Y_1 \\ \vdots \\ Y_{N-1} \end{pmatrix}, \quad \vec{R}^{N+3} = \begin{pmatrix} 1 \\ u + Ac \\ v + Bc \\ H + \hat{u}c \\ Y_1 \\ \vdots \\ Y_{N-1} \end{pmatrix} \quad (8)$$

where

$$q^2 = u^2 + v^2, \quad \hat{u} = Au + Bv \quad (9)$$

$$c = \sqrt{p_\rho + \frac{p p_e}{\rho^2}}, \qquad H = \frac{E + p}{\rho}, \quad (10)$$

$$b_1 = \frac{p_e}{\rho c^2}, \qquad b_2 = 1 + b_1 q^2 - b_1 H, \quad (11)$$

$$b_3 = b_1 \sum_{i=1}^{N-1} Y_i z_i, \qquad z_i = \frac{-p_{Y_i}}{p_e}. \quad (12)$$

3 Pressure Evolution Equation

In order to apply a nonconservative correction to the conservative energy, Karni [5] solves an extra partial differential equation for the pressure which is derived from the equation of state. We will derive this equation for the general equation of state $p = p(\rho, e, Y_1, \cdots, Y_{N-1})$ where the corresponding partial derivatives are denoted by p_ρ, p_e and p_{Y_i}.

We have

$$\frac{Dp}{Dt} = p_\rho \frac{D\rho}{Dt} + p_e \frac{De}{Dt} + \sum_{i=1}^{N-1} \left(p_{Y_i} \frac{DY_i}{Dt} \right) \tag{13}$$

as the convective derivative of the pressure from the chain rule. Simple analysis of the two dimensional Euler Equations in the previous section shows that

$$\rho_t + u\rho_x + v\rho_y = -\rho(u_x + v_y) \tag{14}$$

$$u_t + uu_x + vu_y = -\frac{p_x}{\rho} \tag{15}$$

$$v_t + uv_x + vv_y = -\frac{p_y}{\rho} \tag{16}$$

$$e_t + ue_x + ve_y = -\frac{p}{\rho}(u_x + v_y) \tag{17}$$

$$(Y_i)_t + u(Y_i)_x + v(Y_i)_y = 0 \tag{18}$$

and thus equation 13 can be rewritten as

$$p_t + up_x + vp_y = -\rho(u_x + v_y) \left(p_\rho + \frac{pp_e}{\rho^2} \right) \tag{19}$$

which is equivalent to

$$p_t + up_x + \rho c^2 u_x + vp_y + \rho c^2 v_y = 0 \tag{20}$$

using the definition of the sound speed c given in the previous section.

In some formulations of the equation of state, the pressure can depend on the level set function, ϕ, or on gamma, γ. Since both the level set function and gamma have a vanishing convective derivative,

$$\phi_t + u\phi_x + v\phi_y = 0 \tag{21}$$

$$\gamma_t + u\gamma_x + v\gamma_y = 0 \tag{22}$$

they will both drop out of the pressure evolution equation, just as Y_i, leaving equation 20 unchanged.

Note that the pressure evolution equation reduces to the more familiar form

$$p_t + up_x + \gamma p u_x + vp_y + \gamma p v_y = 0 \tag{23}$$

when $c^2 = \frac{\gamma p}{\rho}$ which occurs quite frequently, e.g. see [2].

4 Upwinding the Pressure Evolution Equation

To get a sense of the upwind discretization of equation 20, we rewrite it as the last equation of a quasilinear system,

$$\begin{pmatrix} u \\ v \\ p \end{pmatrix}_t + \begin{pmatrix} u & 0 & \frac{1}{\rho} \\ 0 & u & 0 \\ \rho c^2 & 0 & u \end{pmatrix} \begin{pmatrix} u \\ v \\ p \end{pmatrix}_x + \begin{pmatrix} v & 0 & 0 \\ 0 & v & \frac{1}{\rho} \\ 0 & \rho c^2 & v \end{pmatrix} \begin{pmatrix} u \\ v \\ p \end{pmatrix}_y = 0 \quad (24)$$

where the eigenvalues and eigenvectors for the 3 by 3 matrix associated with convection in the x-direction are

$$\lambda_x^1 = u - c, \quad \lambda_x^2 = u, \quad \lambda_x^3 = u + c \quad (25)$$

$$\vec{L}_x^1 = \left(\frac{1}{2}, 0, \frac{-1}{2\rho c}\right), \quad \vec{L}_x^2 = (0, 1, 0), \quad \vec{L}_x^3 = \left(\frac{1}{2}, 0, \frac{1}{2\rho c}\right) \quad (26)$$

$$\vec{R}_x^1 = \begin{pmatrix} 1 \\ 0 \\ -\rho c \end{pmatrix}, \quad \vec{R}_x^1 = \begin{pmatrix} 0 \\ 1 \\ 0 \end{pmatrix}, \quad \vec{R}_x^1 = \begin{pmatrix} 1 \\ 0 \\ \rho c \end{pmatrix} \quad (27)$$

and the eigenvalues and eigenvectors for the 3 by 3 matrix associated with convection in the y-direction are

$$\lambda_y^1 = v - c, \quad \lambda_y^2 = v, \quad \lambda_y^3 = v + c \quad (28)$$

$$\vec{L}_y^1 = \left(0, \frac{1}{2}, \frac{-1}{2\rho c}\right), \quad \vec{L}_y^2 = (1, 0, 0), \quad \vec{L}_y^3 = \left(0, \frac{1}{2}, \frac{1}{2\rho c}\right) \quad (29)$$

$$\vec{R}_y^1 = \begin{pmatrix} 0 \\ 1 \\ -\rho c \end{pmatrix}, \quad \vec{R}_y^1 = \begin{pmatrix} 1 \\ 0 \\ 0 \end{pmatrix}, \quad \vec{R}_y^1 = \begin{pmatrix} 0 \\ 1 \\ \rho c \end{pmatrix}. \quad (30)$$

These allow us to rewrite equation 24 as

$$\begin{pmatrix} u \\ v \\ p \end{pmatrix}_t + \sum_{i=1}^{3} \left(\lambda_x^i \vec{R}_x^i \vec{L}_x^i\right) \begin{pmatrix} u \\ v \\ p \end{pmatrix}_x + \sum_{i=1}^{3} \left(\lambda_y^i \vec{R}_y^i \vec{L}_y^i\right) \begin{pmatrix} u \\ v \\ p \end{pmatrix}_y = 0 \quad (31)$$

so that each of the 6 terms can be upwinded according to the sign of the eigenvalue in that term.

The last equation in 31 is equivalent to equation 20, with p_x, u_x, p_y, and v_y replaced as follows,

$$p_x = \frac{1}{2}\left(p_x^{u-c} + p_x^{u+c}\right) - \frac{\rho c}{2}\left(u_x^{u-c} - u_x^{u+c}\right) \tag{32}$$

$$u_x = \frac{1}{2}\left(u_x^{u-c} + u_x^{u+c}\right) - \frac{1}{2\rho c}\left(p_x^{u-c} - p_x^{u+c}\right) \tag{33}$$

$$p_y = \frac{1}{2}\left(p_y^{v-c} + p_y^{v+c}\right) - \frac{\rho c}{2}\left(v_y^{v-c} - v_y^{v+c}\right) \tag{34}$$

$$v_y = \frac{1}{2}\left(v_y^{v-c} + v_y^{v+c}\right) - \frac{1}{2\rho c}\left(p_y^{v-c} - p_y^{v+c}\right) \tag{35}$$

where the superscript on each spatial partial derivatives refers to the eigenvalue which determines the upwind direction for the discretization of that spatial partial derivative. (For example, p_x^{u-c} is the spatial derivative of the pressure discretized using the eigenvalue $u - c$ to determine the upwind direction.) A positive eigenvalue indicates that the characteristic information comes from the left, while a negative eigenvalue indicates that the characteristic information comes from the right. If an eigenvalue is identically zero, then equation 31 shows that the spatial derivative does not contribute to the solution, and can be assigned a zero value for practical numerical and algorithmical purposes.

Note that in the case where the eigenvalues agree on the upwind direction (supersonic flow), the two separate spatial derivatives in each set of parenthesis coalesce to a single value. Thus, the second term in each equation vanishes, and equations 32 to 35 merely dictate upwind differencing in the obvious direction.

5 Discretizing the Pressure Evolution Equation

We wish to solve the pressure evolution equation,

$$p_t + up_x + \rho c^2 u_x + vp_y + \rho c^2 v_y = 0 \tag{36}$$

where the following substitutions are made

$$p_x = \frac{1}{2}\left(p_x^{u-c} + p_x^{u+c}\right) - \frac{\rho c}{2}\left(u_x^{u-c} - u_x^{u+c}\right) \tag{37}$$

$$u_x = \frac{1}{2}\left(u_x^{u-c} + u_x^{u+c}\right) - \frac{1}{2\rho c}\left(p_x^{u-c} - p_x^{u+c}\right) \tag{38}$$

$$p_y = \frac{1}{2}\left(p_y^{v-c} + p_y^{v+c}\right) - \frac{\rho c}{2}\left(v_y^{v-c} - v_y^{v+c}\right) \tag{39}$$

$$v_y = \frac{1}{2}\left(v_y^{v-c} + v_y^{v+c}\right) - \frac{1}{2\rho c}\left(p_y^{v-c} - p_y^{v+c}\right) \tag{40}$$

in order properly upwind the equation. For each grid point i, we need to discretize each of the spatial derivatives on the right hand side of equations 37 to 40 according to the upwind direction determined by the superscript eigenvalue. Once this is done we can evaluate the rest of the terms at i and advance in time.

We will consider the x-direction spatial derivatives (after which the y-direction spatial derivatives become obvious). Consider a variable V with upwind direction determined by an eigenvalue λ. We use polynomial interpolation to find V^λ and then differentiate to get V_x^λ.

The zeroth order divided differences, D_i^0, and all higher order *even* divided differences of V exist at the grid points and will have the subscript i. The first order divided differences, $D_{i+\frac{1}{2}}^1$, and all higher order *odd* divided differences of V exist at the cell walls and will have the subscript $i \pm \frac{1}{2}$.

Consider a specific grid point i_0. If $\lambda_{i_0} = 0$, then setting $(V_x^\lambda)_{i_0} = 0$ will be algorithmically correct as previously discussed, otherwise λ_{i_0} determines the upwind direction. If $\lambda_{i_0} > 0$, then $k = i_0 - 1$. If $\lambda_{i_0} < 0$, then $k = i_0$.

Define

$$Q_1(x) = (D^1_{k+\frac{1}{2}}V)(x - x_{i_0}). \tag{41}$$

If $|D^2_k V| \leq |D^2_{k+1}V|$, then $s = D^2_k V$ and $k^\star = k - 1$. Otherwise, $s = D^2_{k+1}V$ and $k^\star = k$. Define

$$Q_2(x) = s(x - x_k)(x - x_{k+1}). \tag{42}$$

If $|D^3_{k^\star - \frac{1}{2}}V| \leq |D^3_{k^\star + \frac{1}{2}}V|$, then $s^\star = D^3_{k^\star - \frac{1}{2}}V$. Otherwise, $s^\star = D^3_{k^\star + \frac{1}{2}}V$. Define

$$Q_3(x) = s^\star(x - x_{k^\star})(x - x_{k^\star+1})(x - x_{k^\star+2}). \tag{43}$$

And then $(V^\lambda_x)_{i_0}$ is

$$D^1_{k+\frac{1}{2}}V + s\left(2(i_0 - k) - 1\right)\triangle x + s^\star\left(3(i_0 - k^\star)^2 - 6(i_0 - k^\star) + 2\right)(\triangle x)^2. \tag{44}$$

This is a third order upwind spatial discretization. For a second order upwind spatial discretization, only keep the first two terms in equation 44. For a first order upwind spatial discretization, only keep the first term in equation 44 (standard upwinding).

(Note that we do not use the special viscosity discussed in [6], although it could be added to the quasilinear system, and the modified system could discretized in a fashion similar to the one outlined above.)

6 Modification of the Conservative Solver

In order to solve the two dimensional Euler equations, we utilize a fully conservative high order algorithm as outlined in [2] and [3]. While adequate for many problems, the conservative solver will occasionally yield large nonphysical oscillations and we will need to locally apply a nonconservative correction to the total energy in these regions.

Suppose that we have an acceptable smooth solution for the conserved variables and the pressure (from the equation of state) and that we wish to advance to a new time level (or sublevel in the case of Runge-Kutta methods). The conservative scheme will give us new values for the conserved variables and these in turn give us a new pressure (from the equation of state). It is this pressure that initiates the oscillations in regions where the interface is numerically ill-conditioned. An alternative pressure can be constructed from the pressure evolution equation, and this new pressure can be used to define a nonconservative energy using the equation of state. Then in regions where the interface is numerically ill-conditioned, we replace the energy computed from the conservative scheme with the nonconserved energy computed from the pressure evolution equation.

There are many way to locate potential problem interfaces. In [5], Karni looks for jumps in the mass fraction or for sign changes in the level set function. In [4], the authors look for regions where both temperature and gamma change sign. In general, this procedure is dependent on the formulation of the problem, and one may want to consider many things, e.g. mass fractions, level sets, gamma, temperature, and equations of state. The conservative solution can be compared to the solution obtained with the nonconservative correction method in order to determine which flow features are physically authentic.

7 Examples

We will use the thermally perfect Euler equations for our examples. These will be solved with the standard conservative methods outlined in [2] and [3], along with the CPM [1] which gives an efficient method for eigensystem treatment with no loss of accuracy. When the standard conservative method admits nonphysical oscillations at an interface, we will make a local, nonconservative correction to the total energy. This will be done by solving the pressure evolution equation and applying the equation of state to the resultant pressure to obtain a new energy.

7.1 Example 1

Consider an isolated contact discontinuity separating oxygen and argon. Initially, we set velocity, pressure, and temperature to constant values, forcing a jump in density. Figure 1 shows that the contact moves to the right with no numerical difficulties, even though both gamma and the mass fraction have jumps. However, if we initially set the density to a constant value, forcing a jump in temperature, the conservative scheme admits nonphysical oscillations as shown in figure 2. Application of a local nonconservative correction to the total energy alleviates these oscillations as shown in figure 3. The local correction was applied to about 3 to 5 grid points in the vicinity of the contact.

7.2 Example 2

Consider a one dimensional shock tube problem with argon on the left and oxygen on the right. Both gases are initially at rest, with a jump in both pressure and temperature across the interface that initiates the formation of three waves: a shock wave, a contact discontinuity, and a rarefaction wave. Figure 4 shows that the conservative method works quite well, even though there are jumps in temperature, gamma, and the mass fraction at the interface. The results for the nonconservative correction method are shown in figure 5. The pressure and velocity are somewhat flatter near the contact, but the density and temperature have nonphysical overshoots caused by the

artificial peak in the energy that was introduced by the nonconservative correction.

Figures 6 and 7 show the results on a fine grid. The fully conservative method works fine on this problem and the nonconservative correction method is not needed. In fact, the nonconservative correction method introduces an error near the rarefaction corner, even though it was only applied on a few grid points near the center of the domain.

This example points out that the nonconservative correction method should only be used as a back-up scheme when the fully conservative method breaks down, and that the results obtained should be carefully scrutinized. In addition, since the shock location is fairly accurate, this example serves as a warning to those who perceive the shock location as the only indication of the validity of a nonconservative solution, or as the only reason to use a conservative method.

7.3 Example 3

Consider another shock tube problem, with slightly different initial conditions. The fully conservative method admits small nonphysical oscillations in figure 8 which are fixed by the nonconservative correction method in figure 9. Note that the nonconservative correction method has trouble with the rarefaction corner. Also note that both schemes give a small energy spike near the interface.

Figures 10 and 11 show the two schemes on a fine grid. The conservative scheme is adequate, although the nonconservative correction method gives smoother results near the contact discontinuity. Note that both schemes have a little trouble with the rarefaction corner. More importantly, note that the spike in energy is present in both schemes, and that it appears to be an authentic feature under grid refinement for the fully conservative scheme. However, this spike in total energy seems to lack physical relevance since the temperature is monotone in the region and pressure and velocity are constant.

7.4 Example 4

In this example, we only have one gas: oxygen (initially at rest). At $x = .4$, we have a pressure and temperature jump that will evolve into 3 waves, one

being a shock headed to the right. At $x = .6$, we have an interface across which the temperature jumps (causing a jump in gamma, since the oxygen is thermally perfect). Figure 12 shows the shock traveling to the right before it hits the interface, while figure 13 shows the solution after the shock passes through the interface. Both figures were obtained with a fully conservative method. Note that the large jump in both temperature and gamma do not cause much difficulty when hit by the shock, possibly because the mass fraction is constant. The nonconservative correction method only slightly improves the solution as shown in figure 14.

7.5 Example 5

Similar to the last example, we set up a shock tube at $x = .4$ and a temperature jump at $x = .6$. In addition, we have argon to the right of $x = .6$ with oxygen to the left. Figure 15 shows the shock traveling to the right before it hits the interface, while figure 16 shows the solution after the shock passes through the interface. Both figures were obtained with a fully conservative method. Figure 17 shows the solution after the shock passes through the interface for the nonconservative correction method. Comparison of figures 16 and 17 indicate that the conservative method admits large nonphysical oscillations. Note that these occurred even though gamma was nearly constant.

Figure 18 and 19 show the solutions obtained on a fine grid. Note that the conservative method still admits nonphysical oscillations which pollute the solution. The nonconservative correction method performs much better, although there are still some minute imperfections in the solution.

7.6 Example 6

Similar to the last example, a shock hits an interface. Figures 20, 21, 22, and 23 show the results.

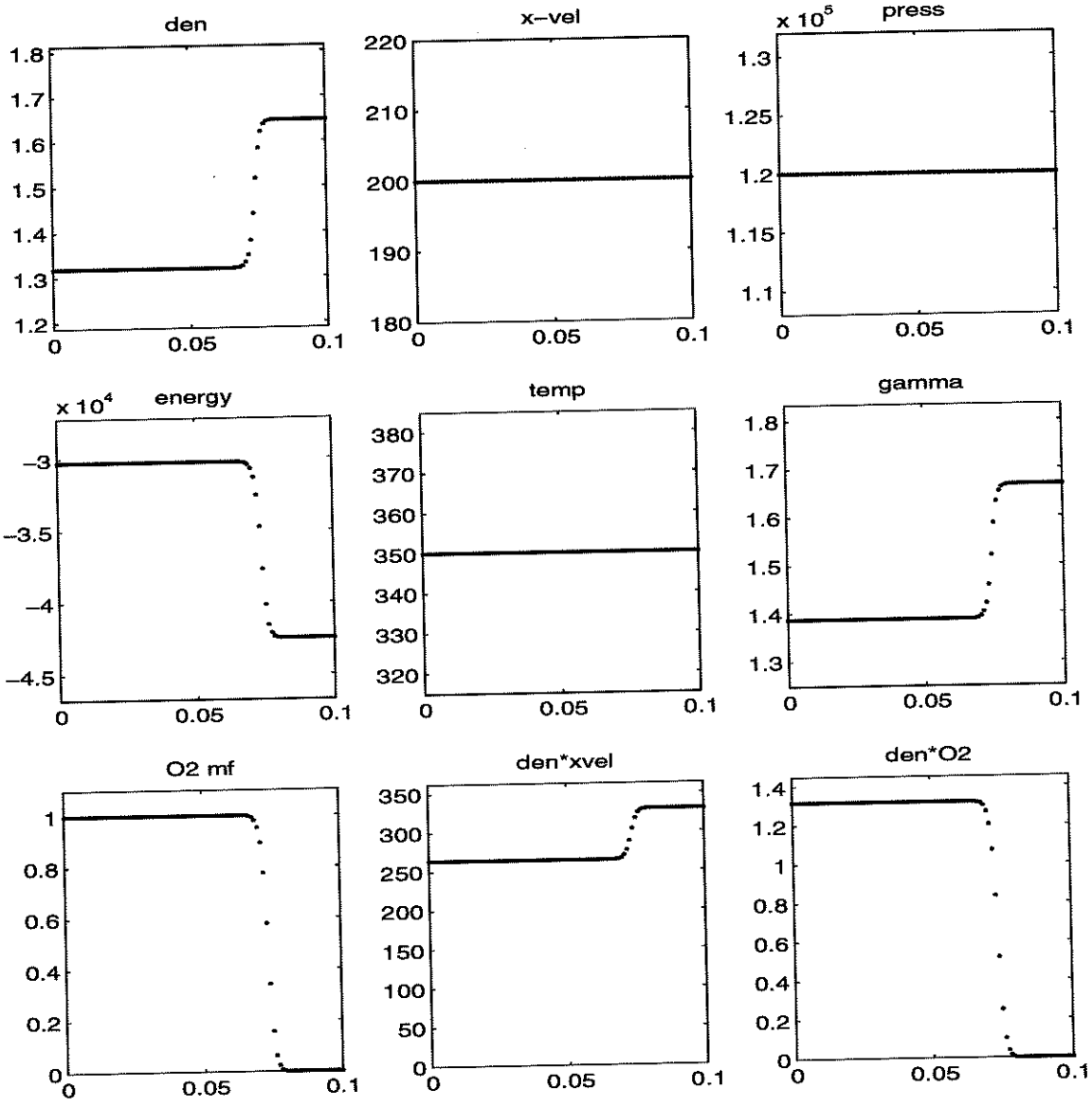

Figure 1: Example 1 - conservative method - contact discontinuity - constant temperature

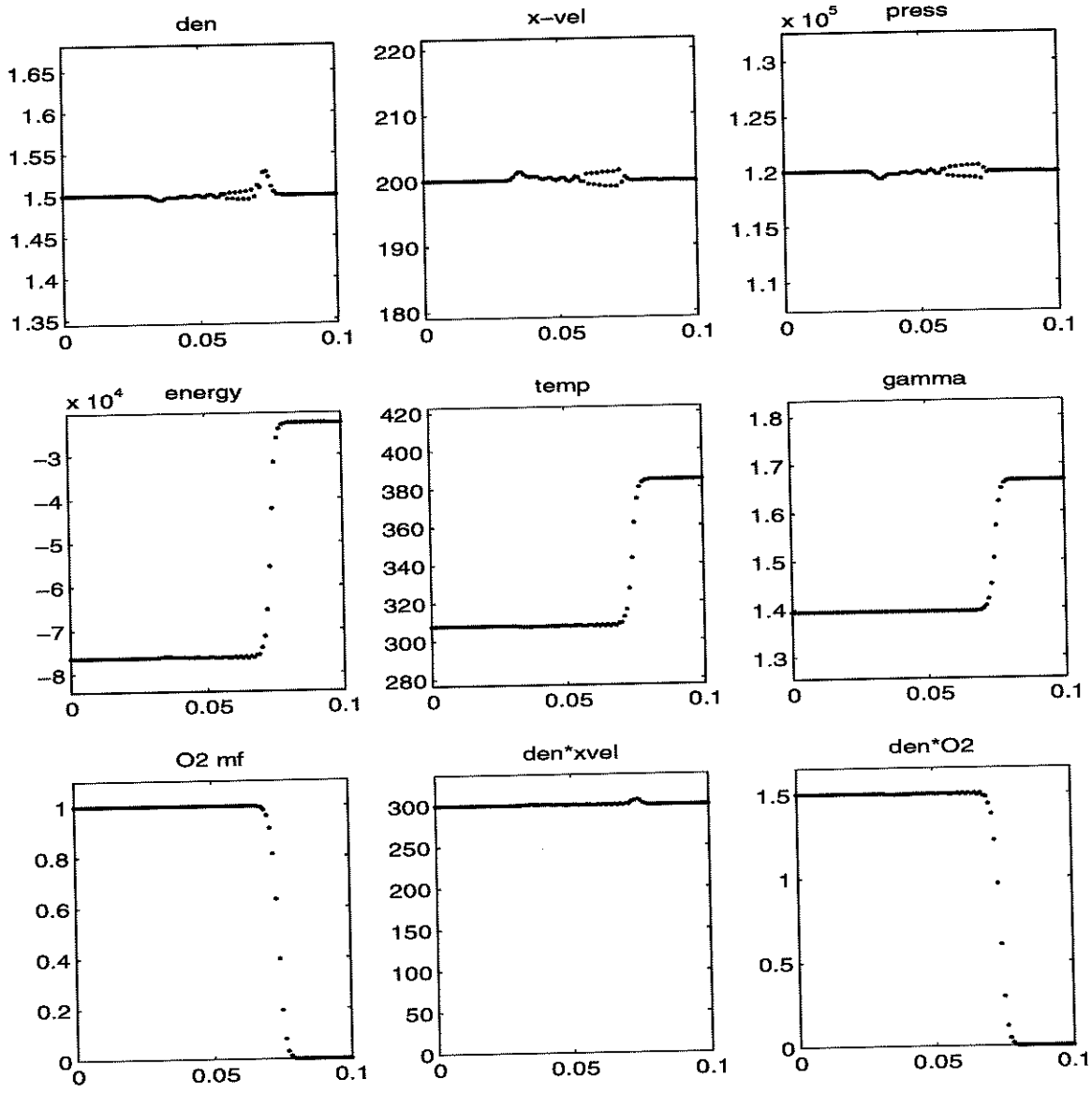

Figure 2: Example 1 - conservative method - contact discontinuity - jump in temperature

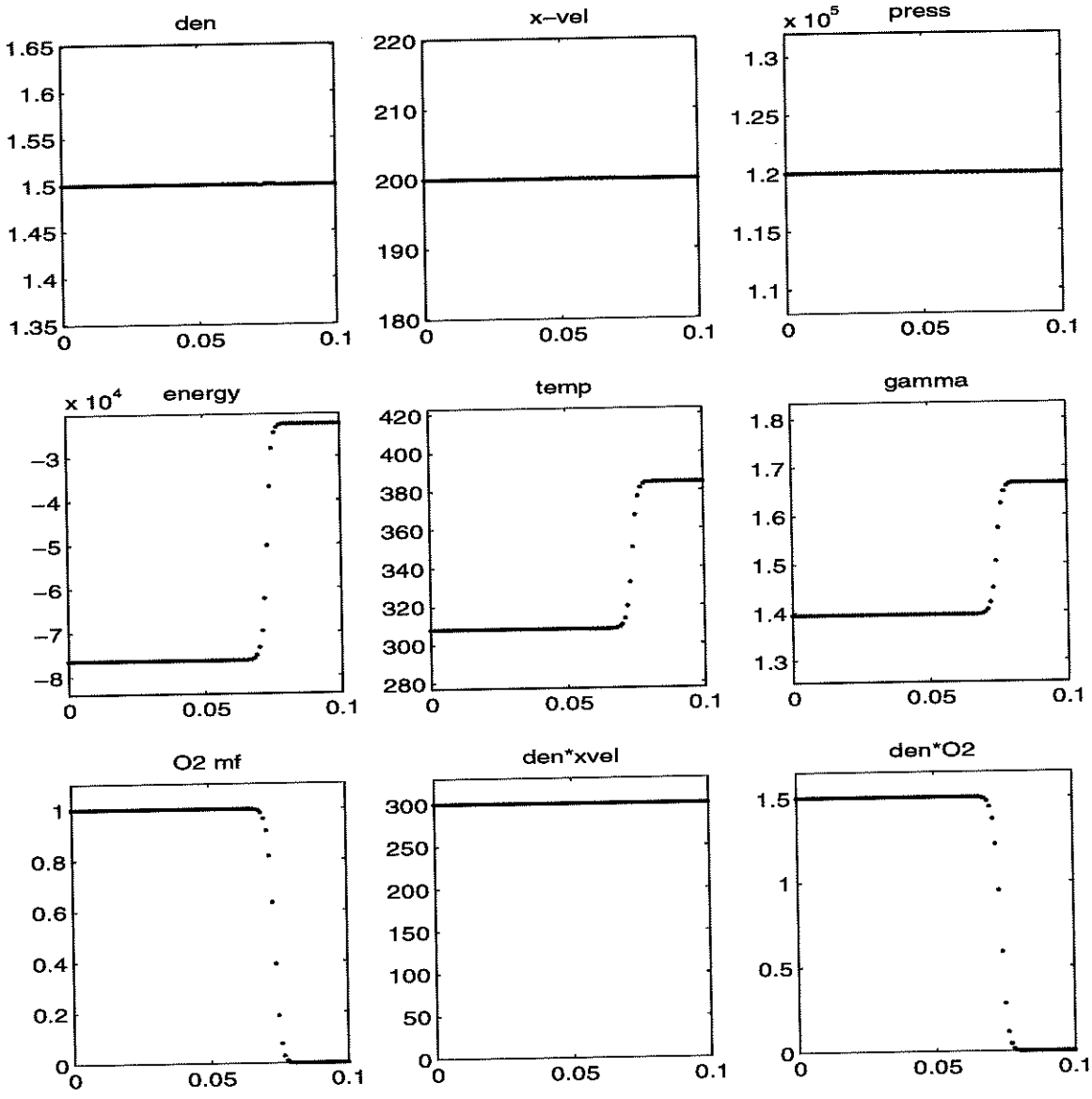

Figure 3: Example 1 - nonconservative correction - contact discontinuity - jump in temperature

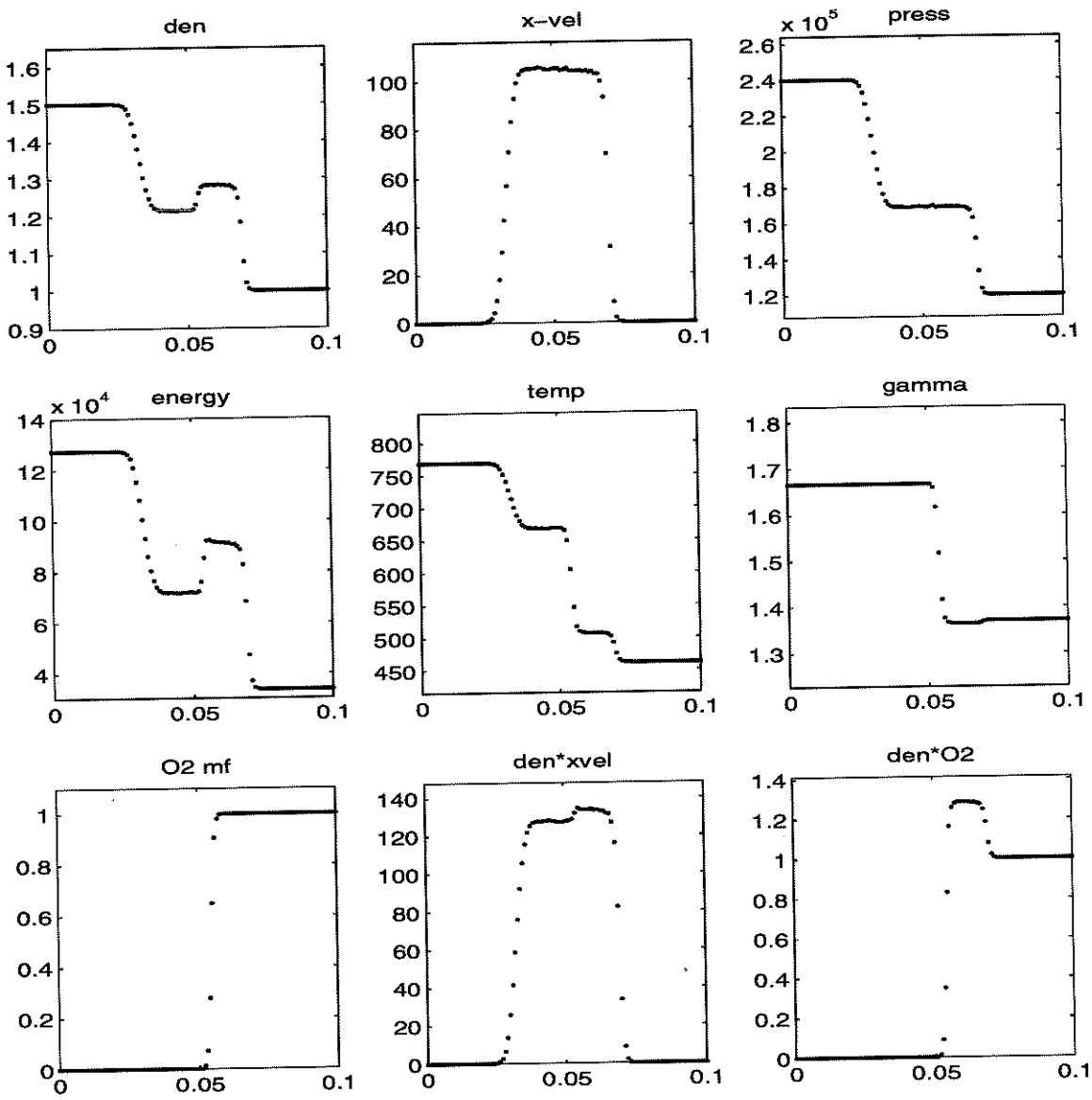

Figure 4: Example 2 - conservative method - shock tube - 100 points

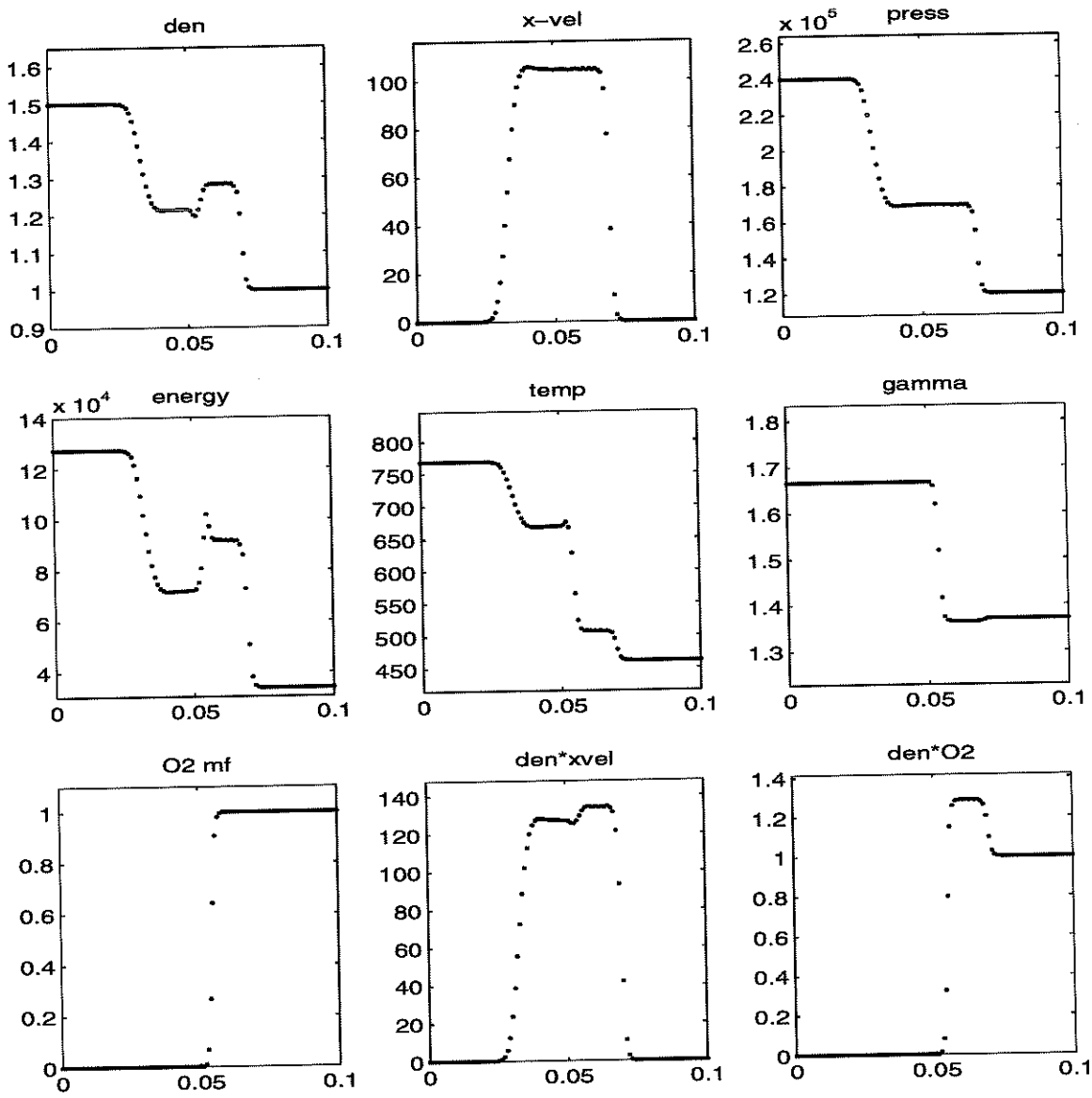

Figure 5: Example 2 - nonconservative correction - shock tube - 100 points

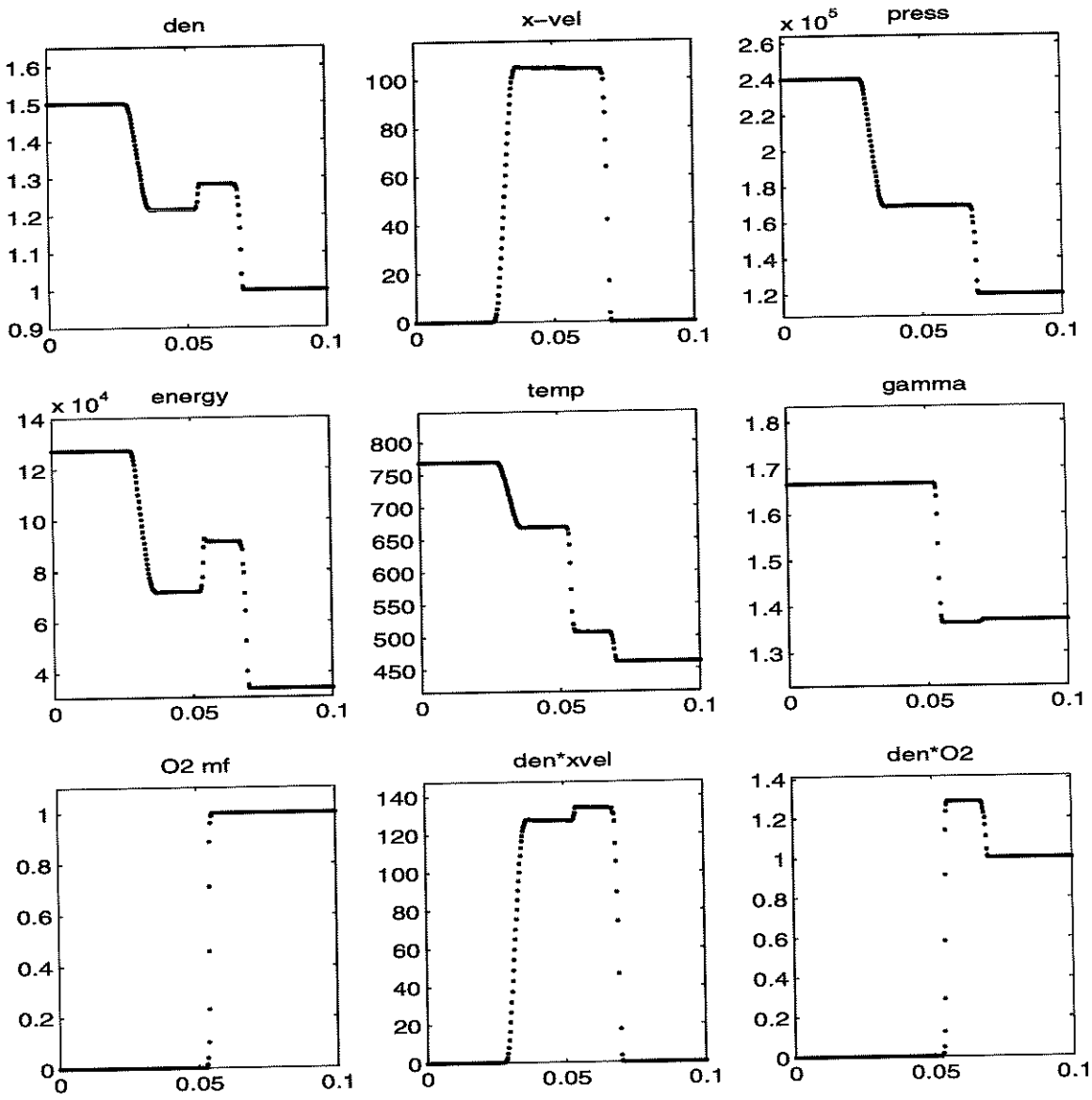

Figure 6: Example 2 - conservative method - shock tube - 400 points

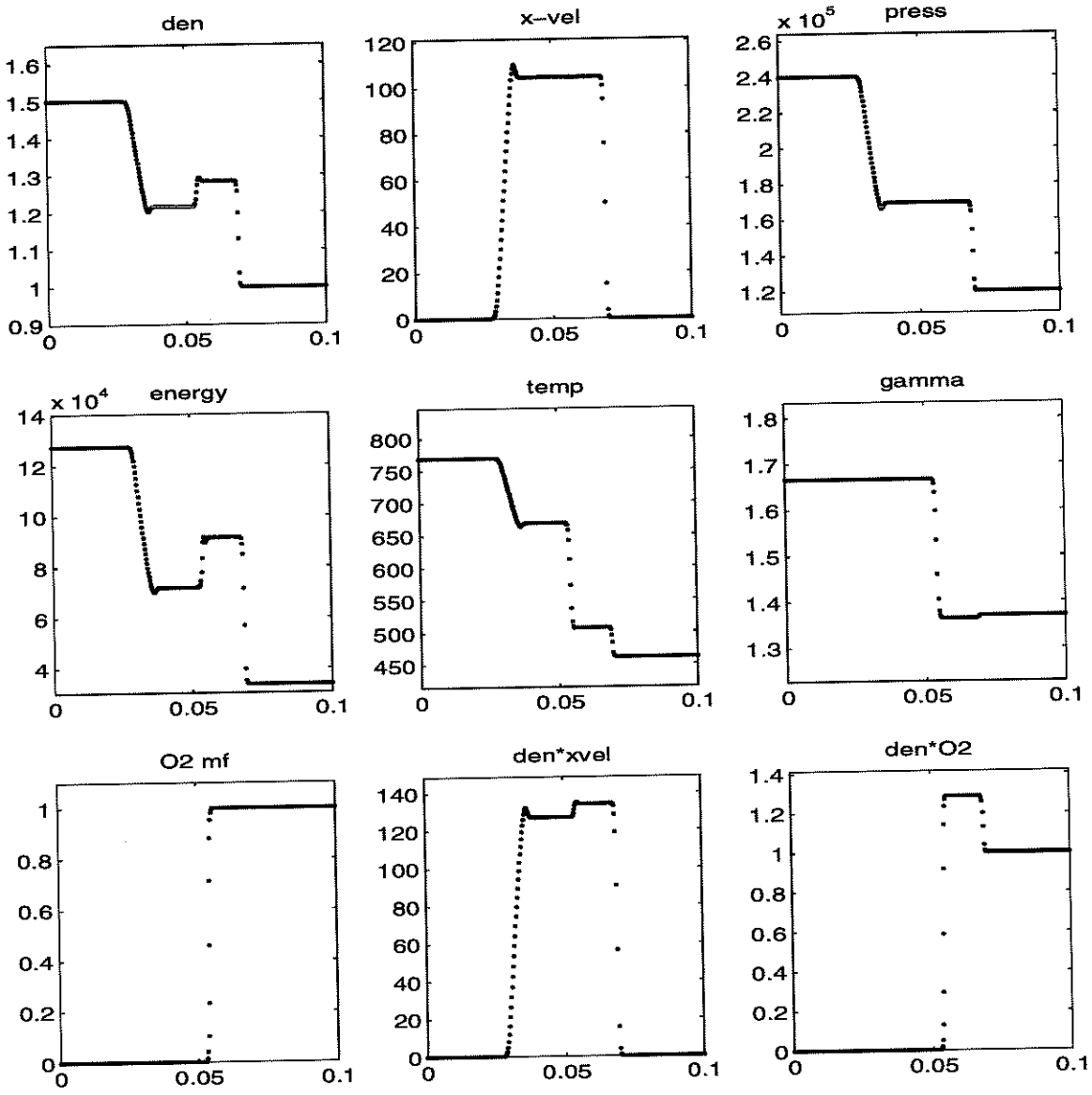

Figure 7: Example 2 - nonconservative correction - shock tube - 400 points

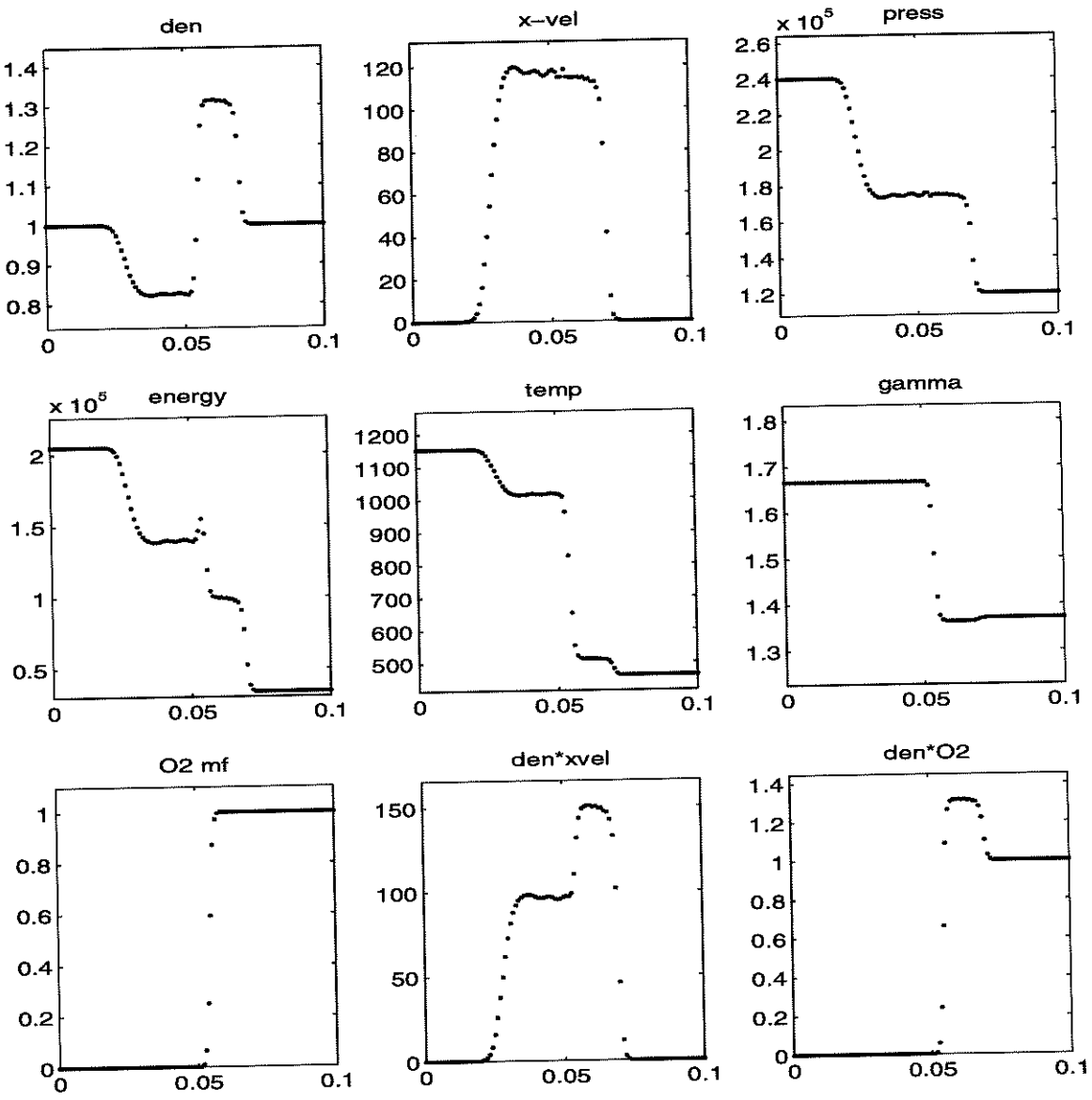

Figure 8: Example 3 - conservative method - shock tube - 100 points

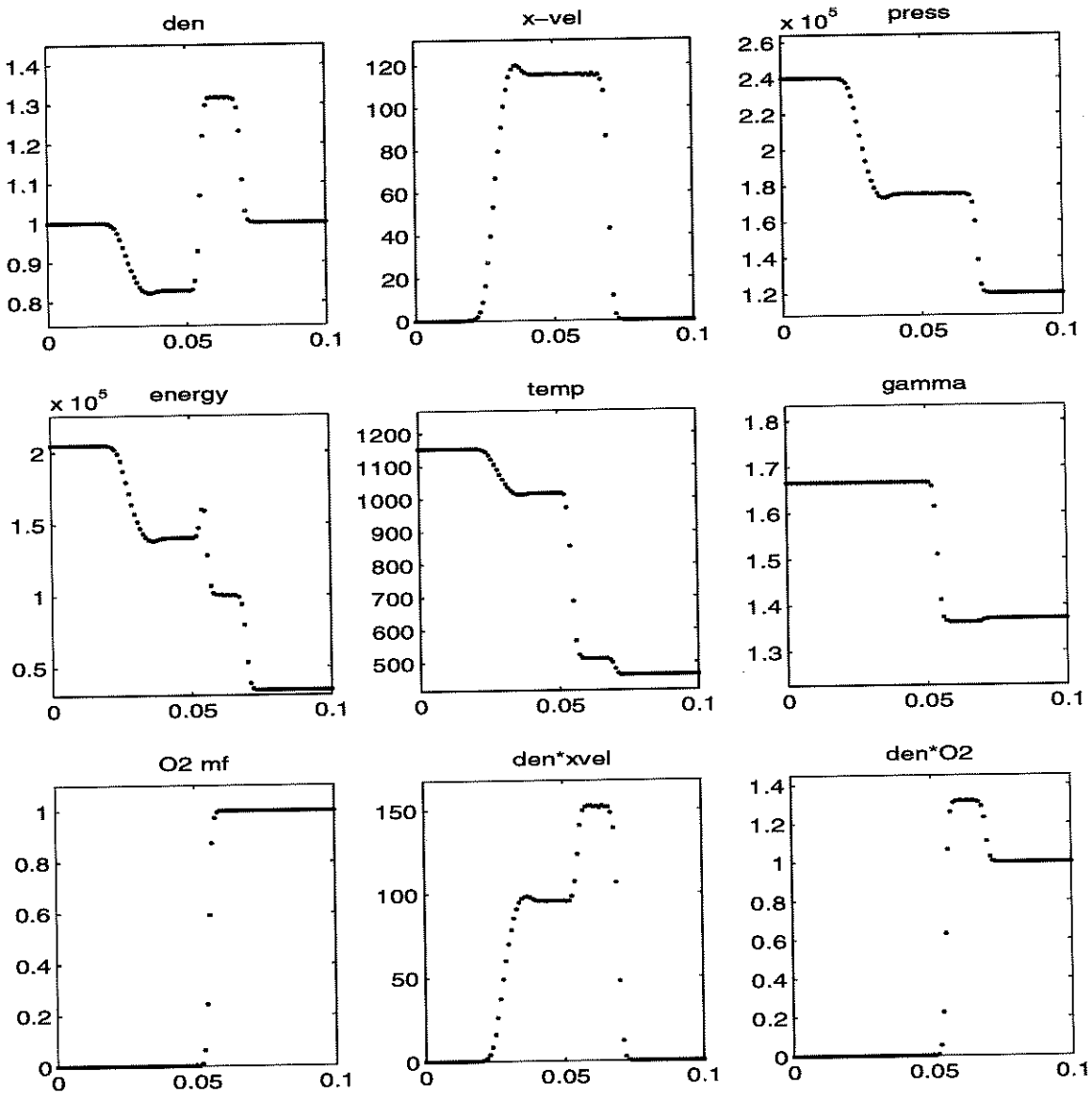

Figure 9: Example 3 - nonconservative correction - shock tube - 100 points

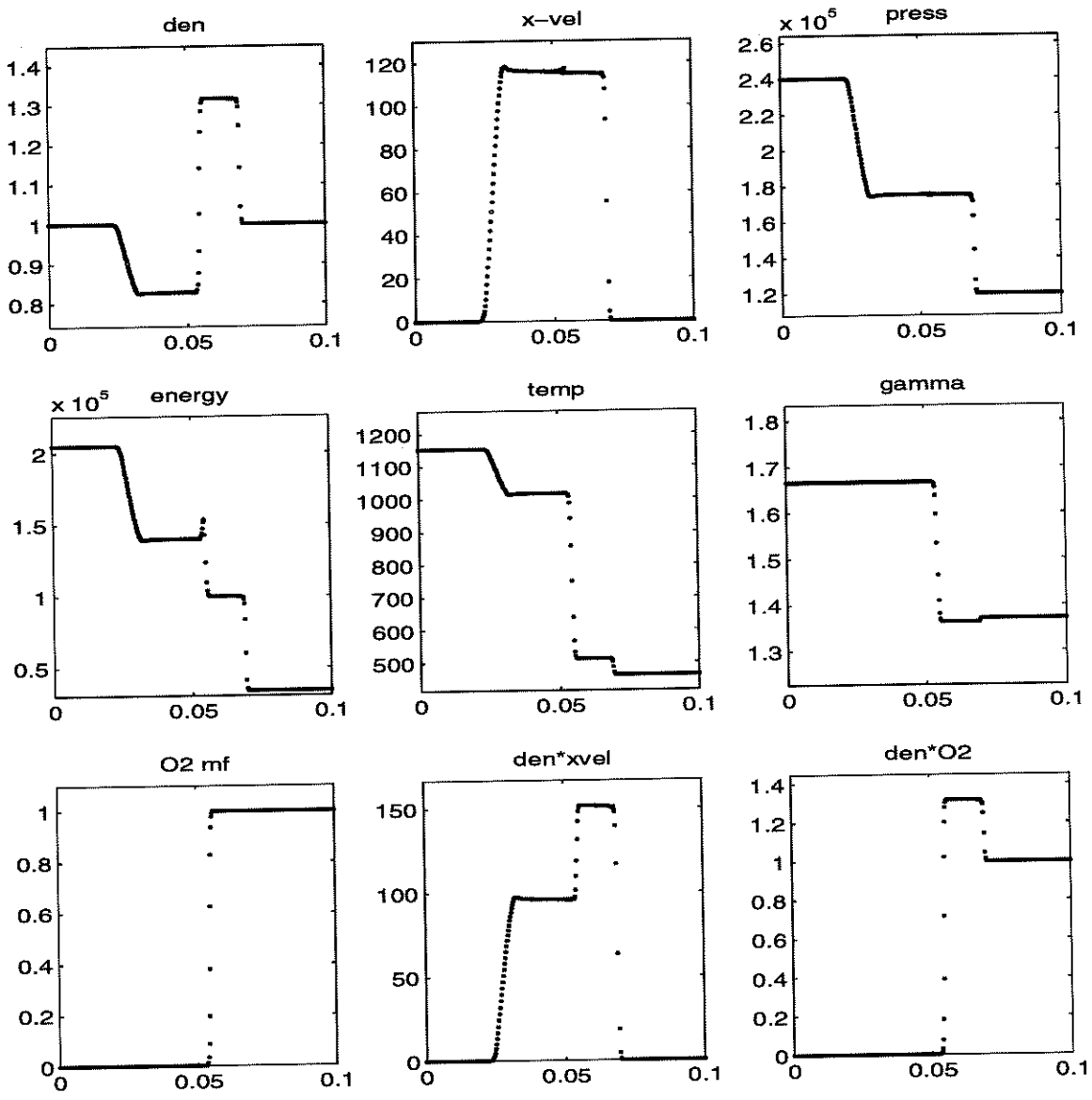

Figure 10: Example 3 - conservative method - shock tube - 400 points

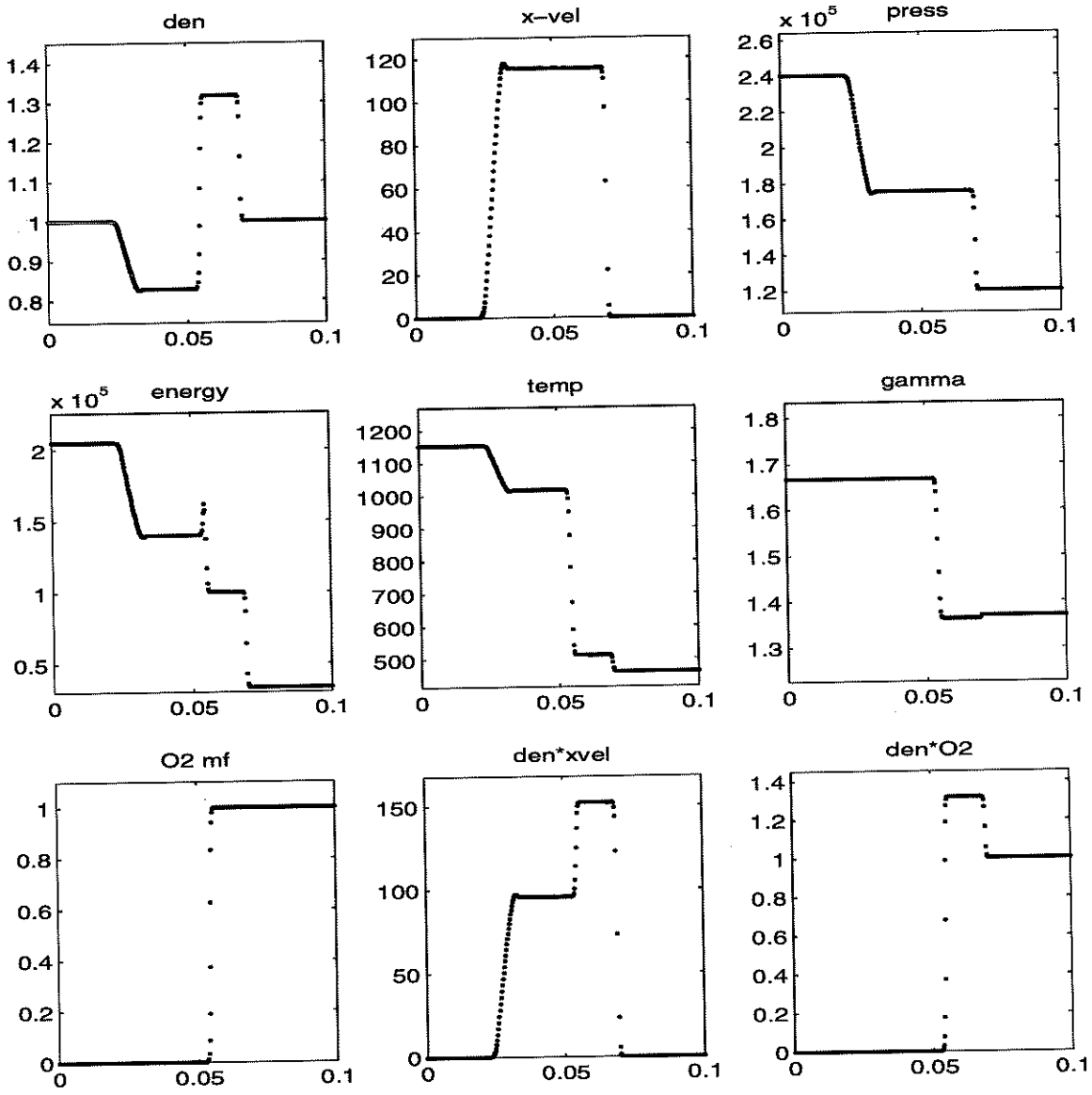

Figure 11: Example 3 - nonconservative correction - shock tube - 400 points

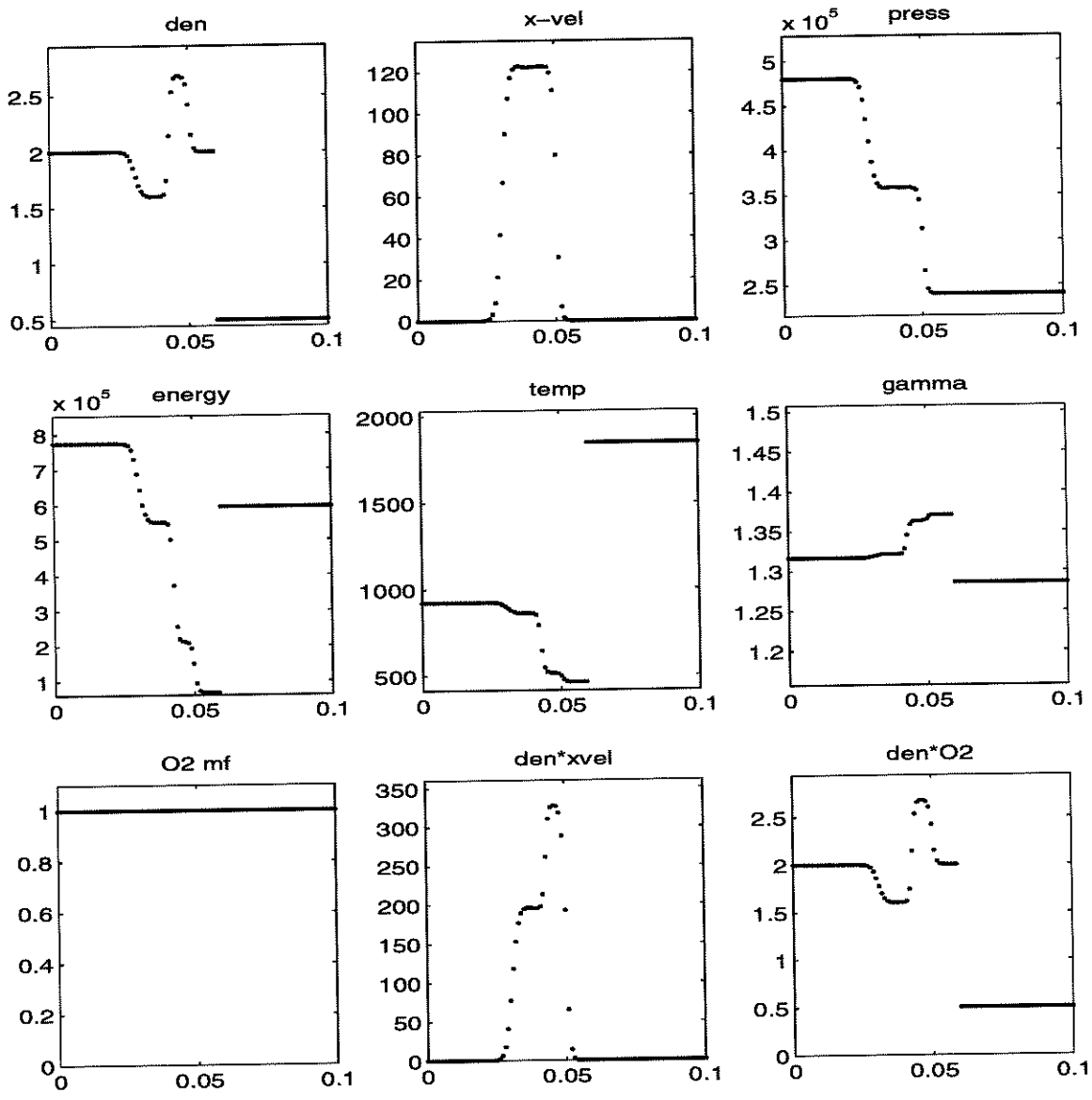

Figure 12: Example 4 - conservative method - before collision

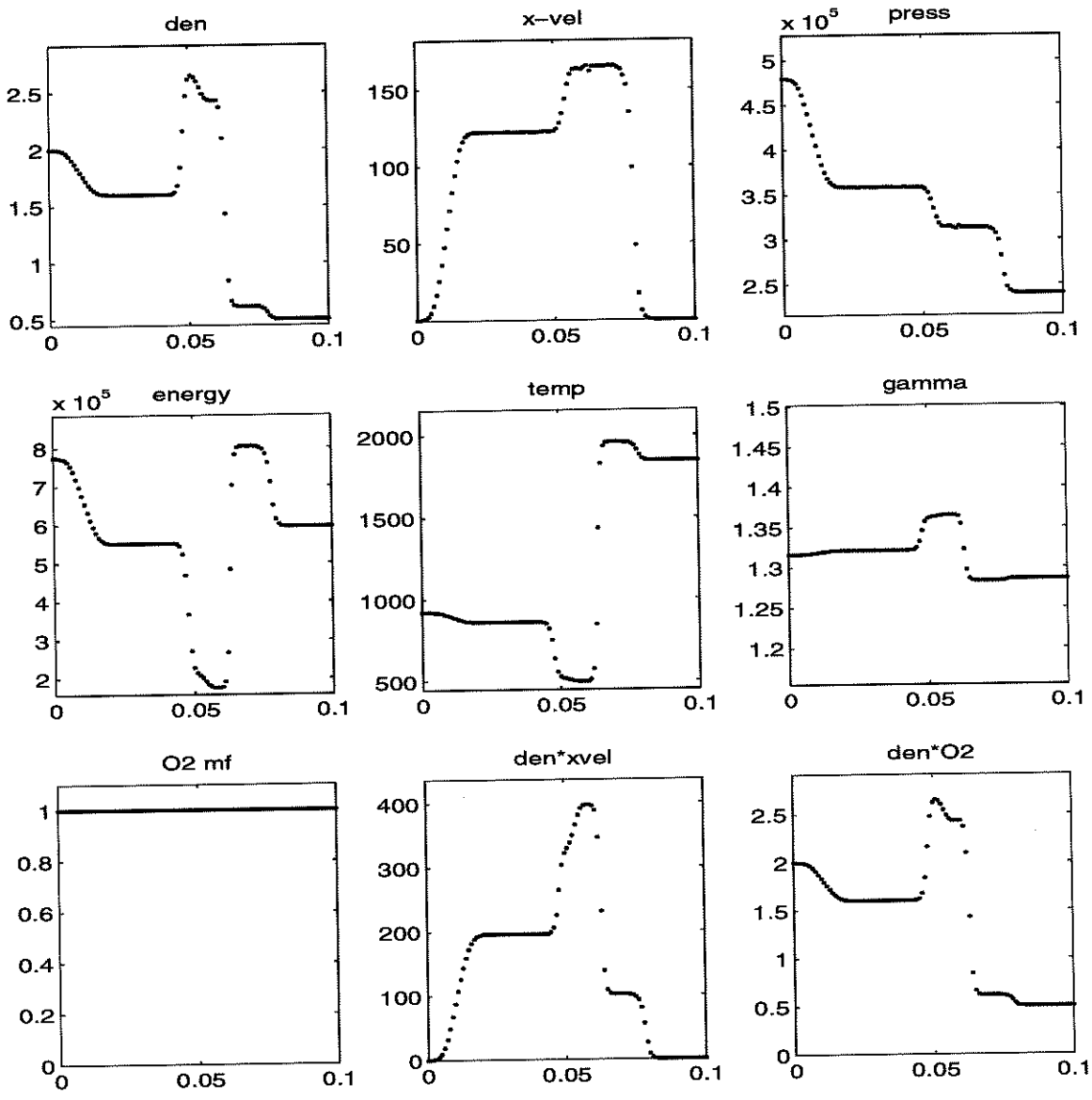

Figure 13: Example 4 - conservative method - after collision

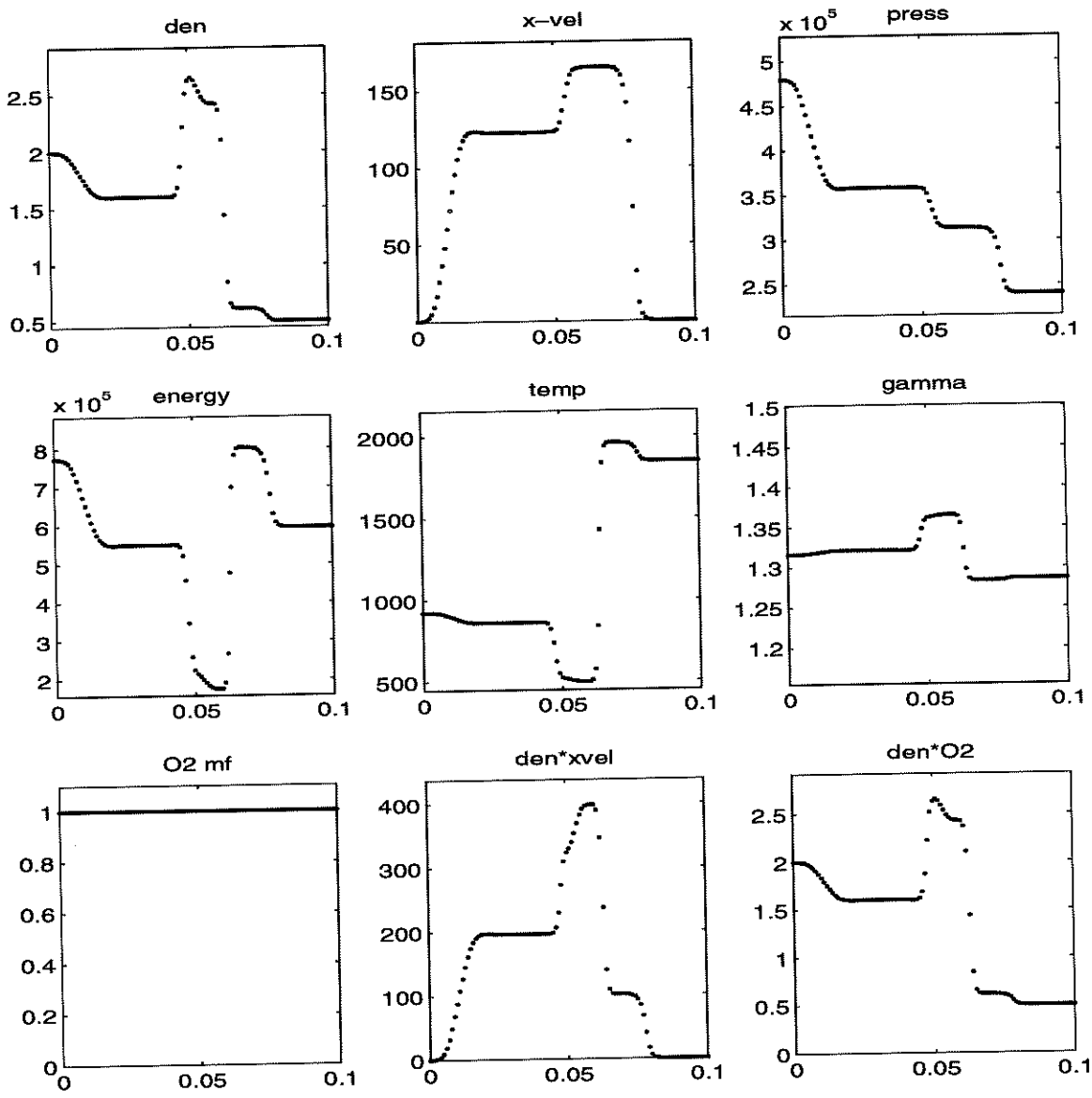

Figure 14: Example 4 - nonconservative correction - after collision

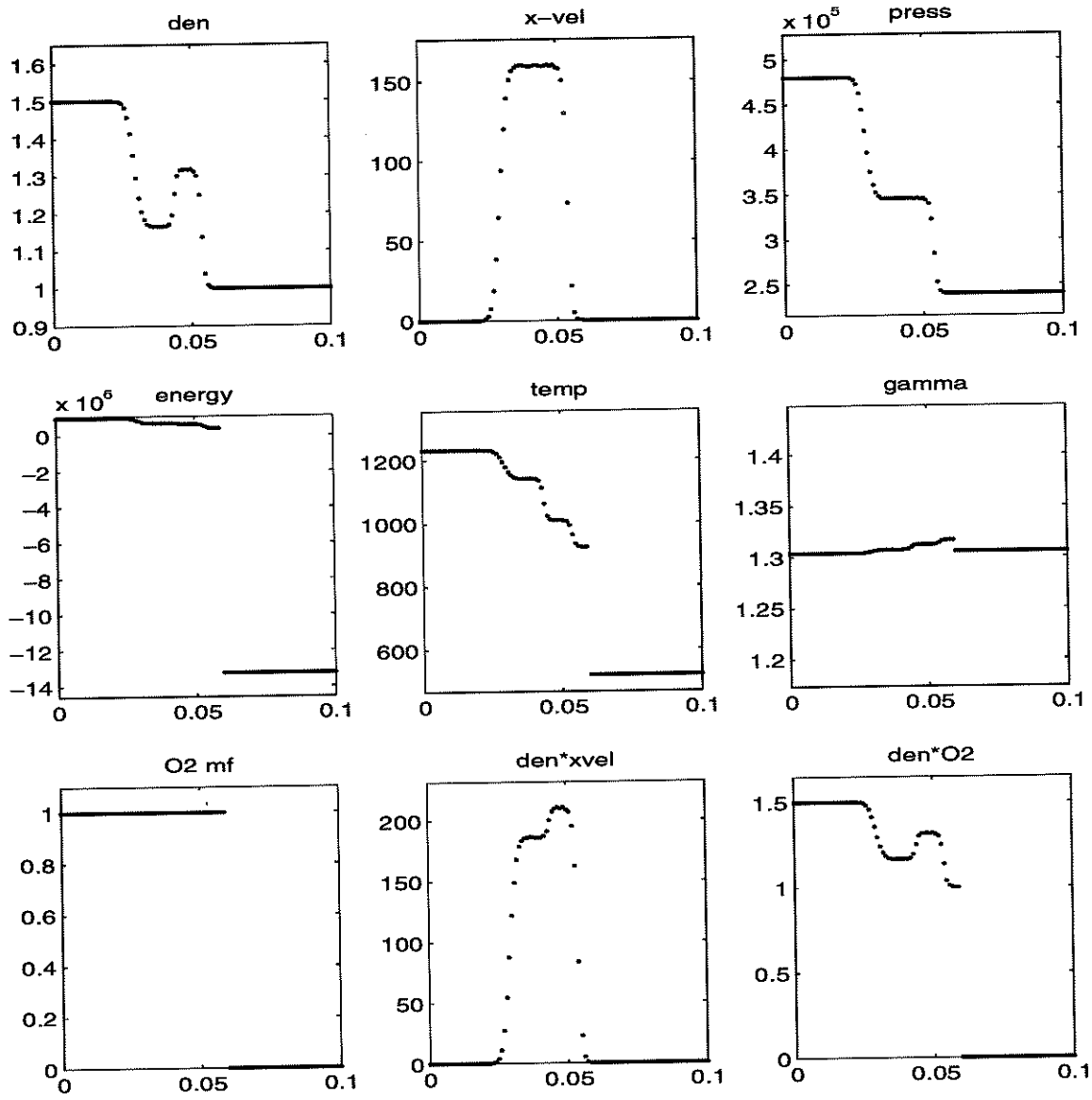

Figure 15: Example 5 - conservative method - before collision - 100 points

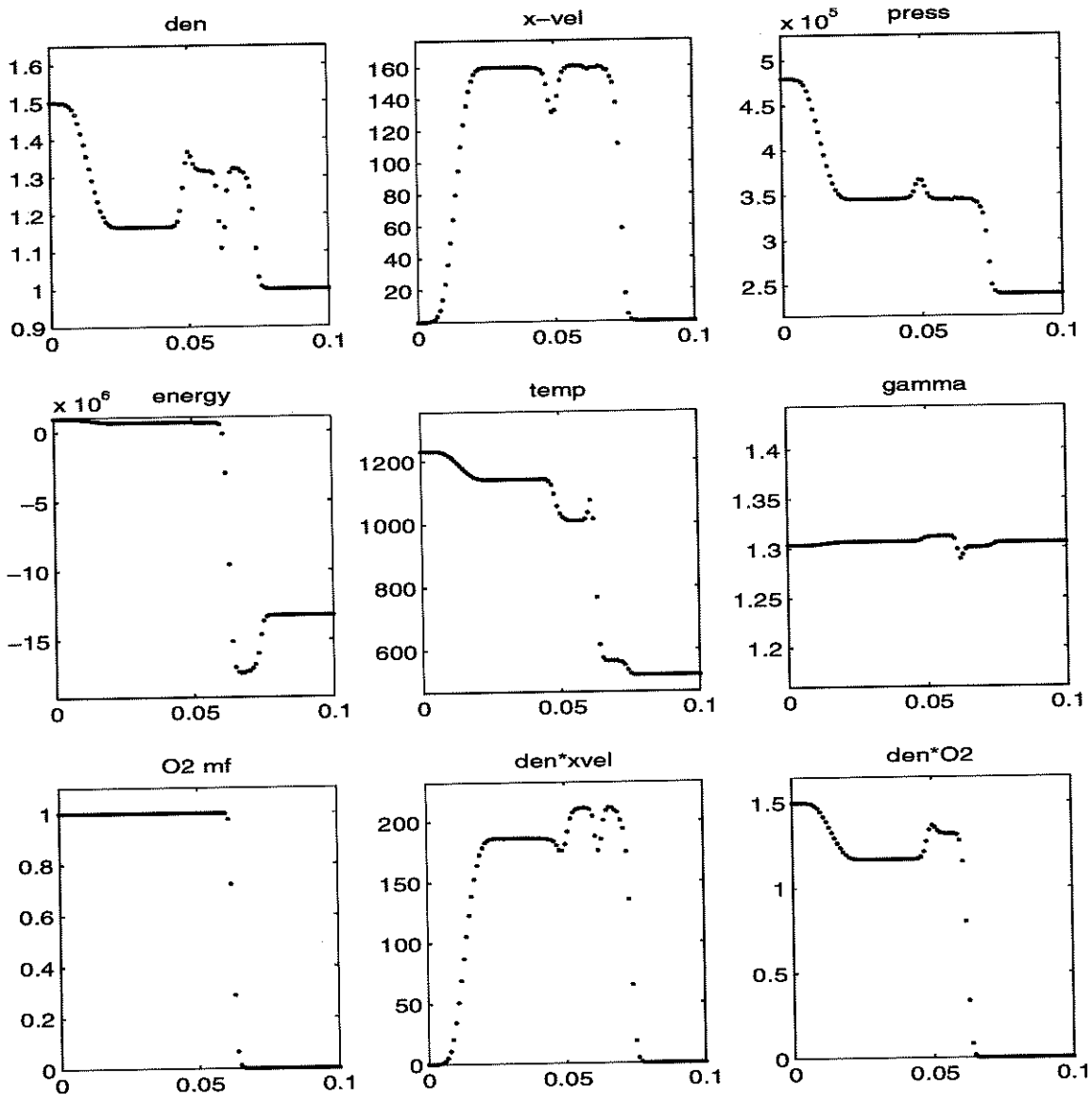

Figure 16: Example 5 - conservative method - after collision - 100 points

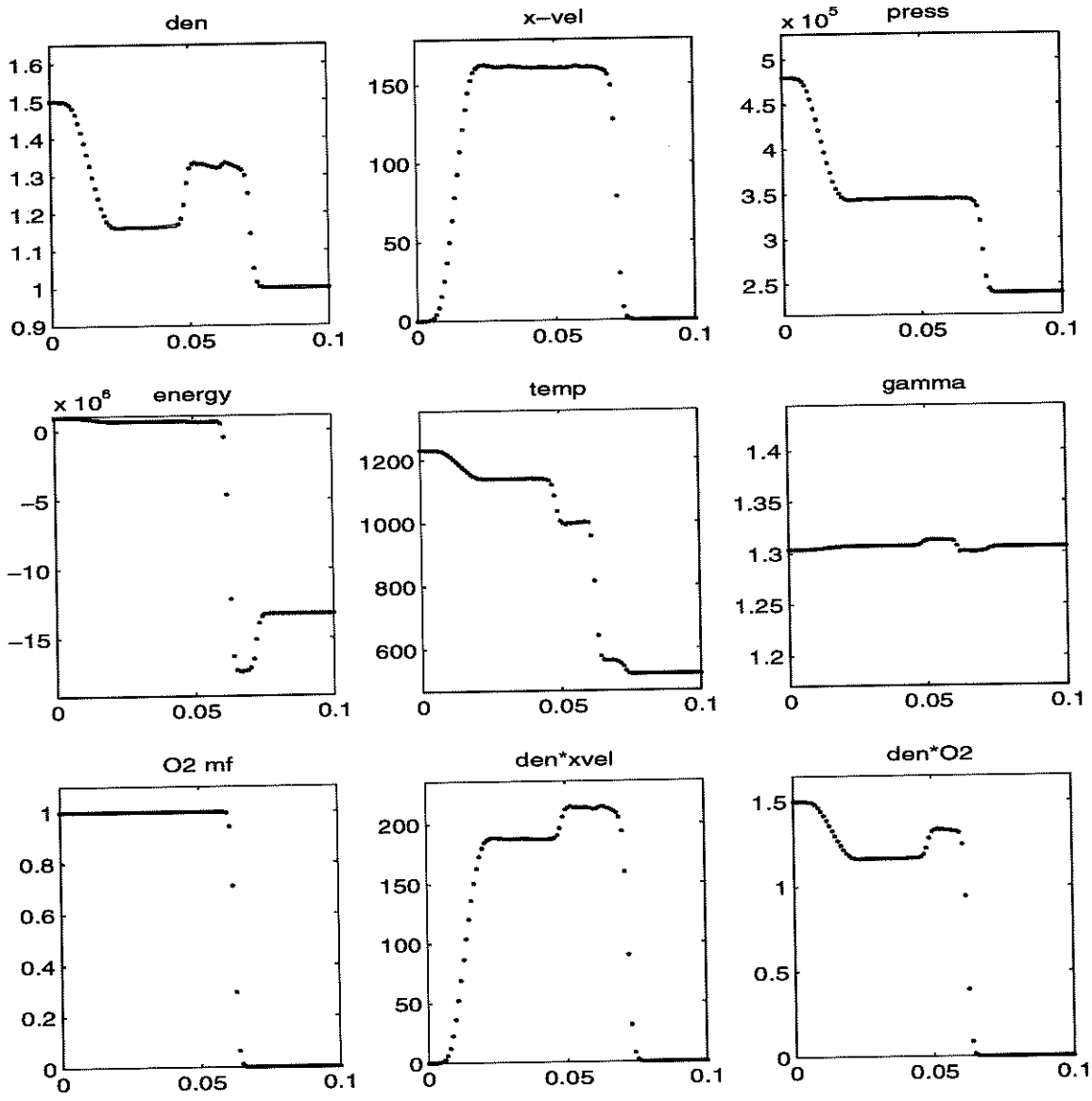

Figure 17: Example 5 - nonconservative correction - after collision - 100 points

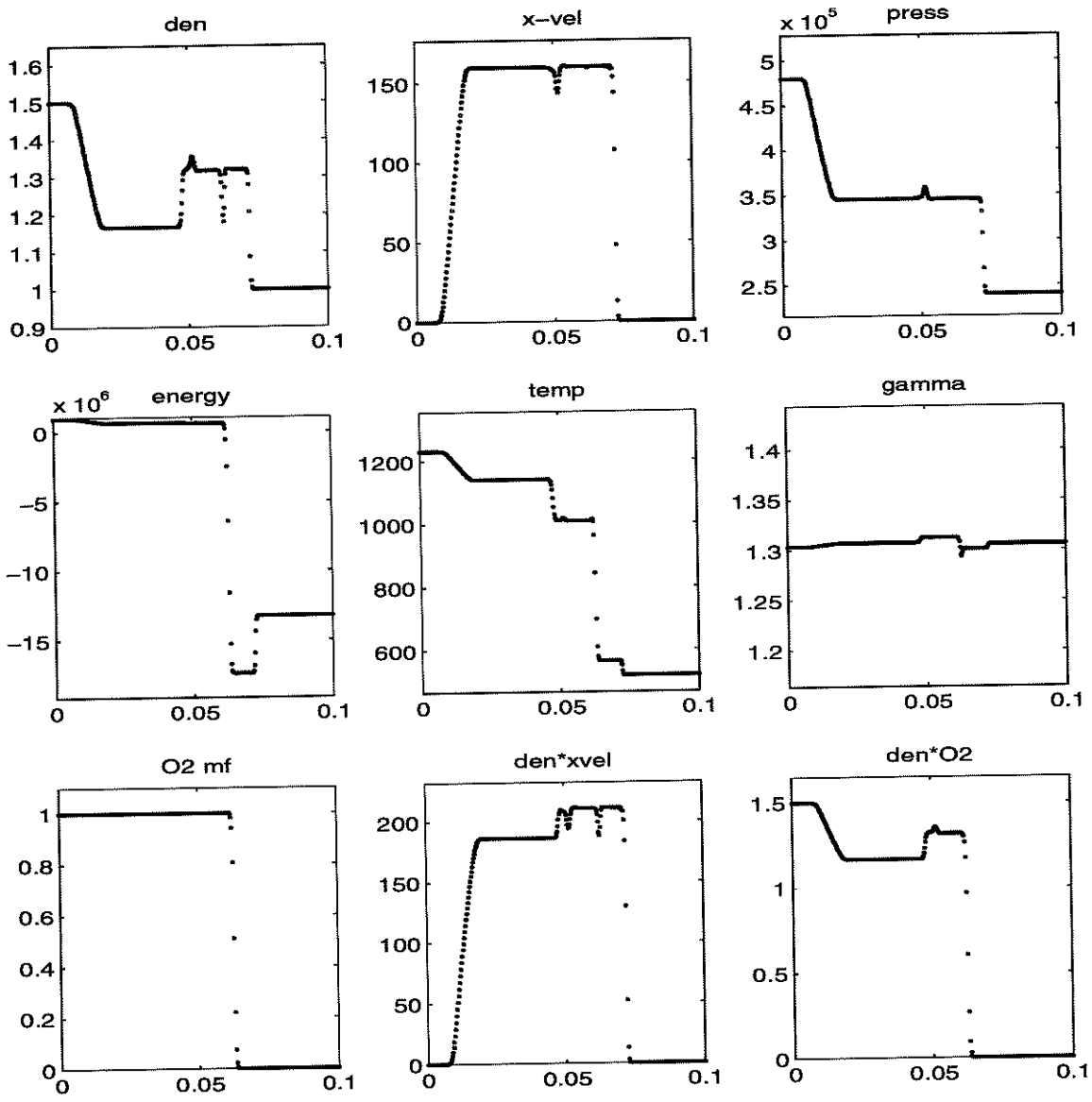

Figure 18: Example 5 - conservative method - after collision - 400 points

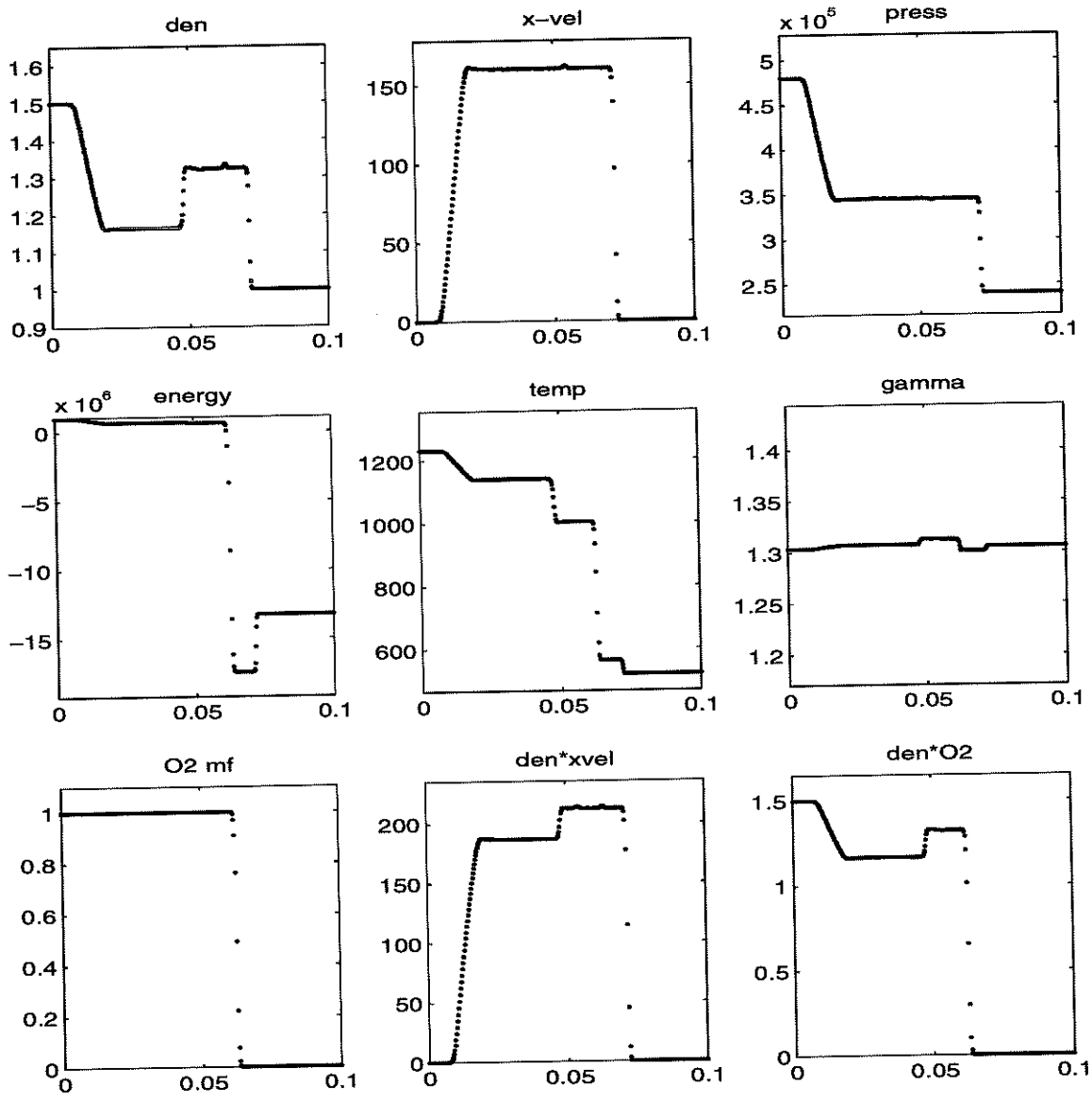

Figure 19: Example 5 - nonconservative correction - after collision - 400 points

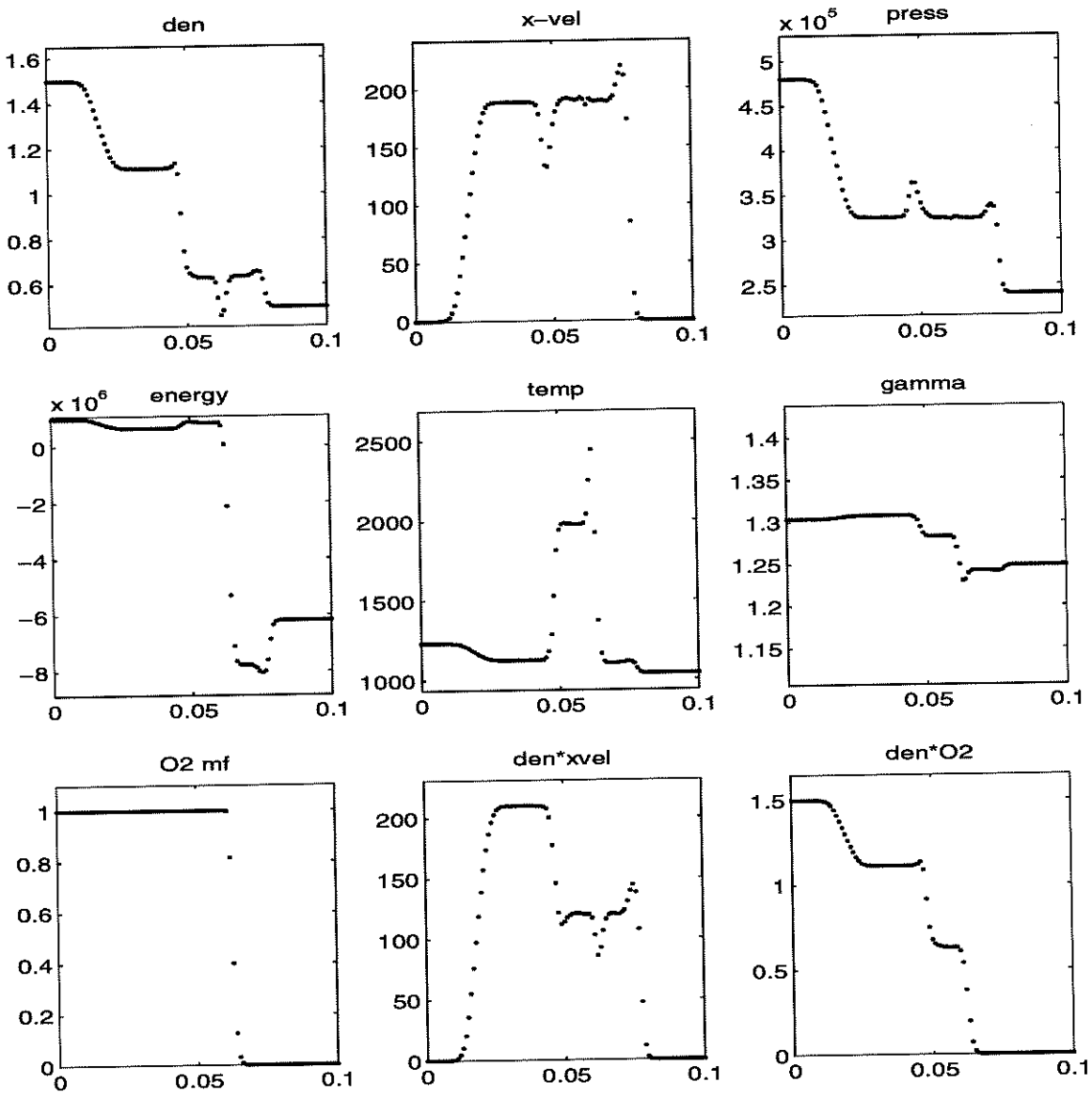

Figure 20: Example 6 - conservative method - after collision - 100 points

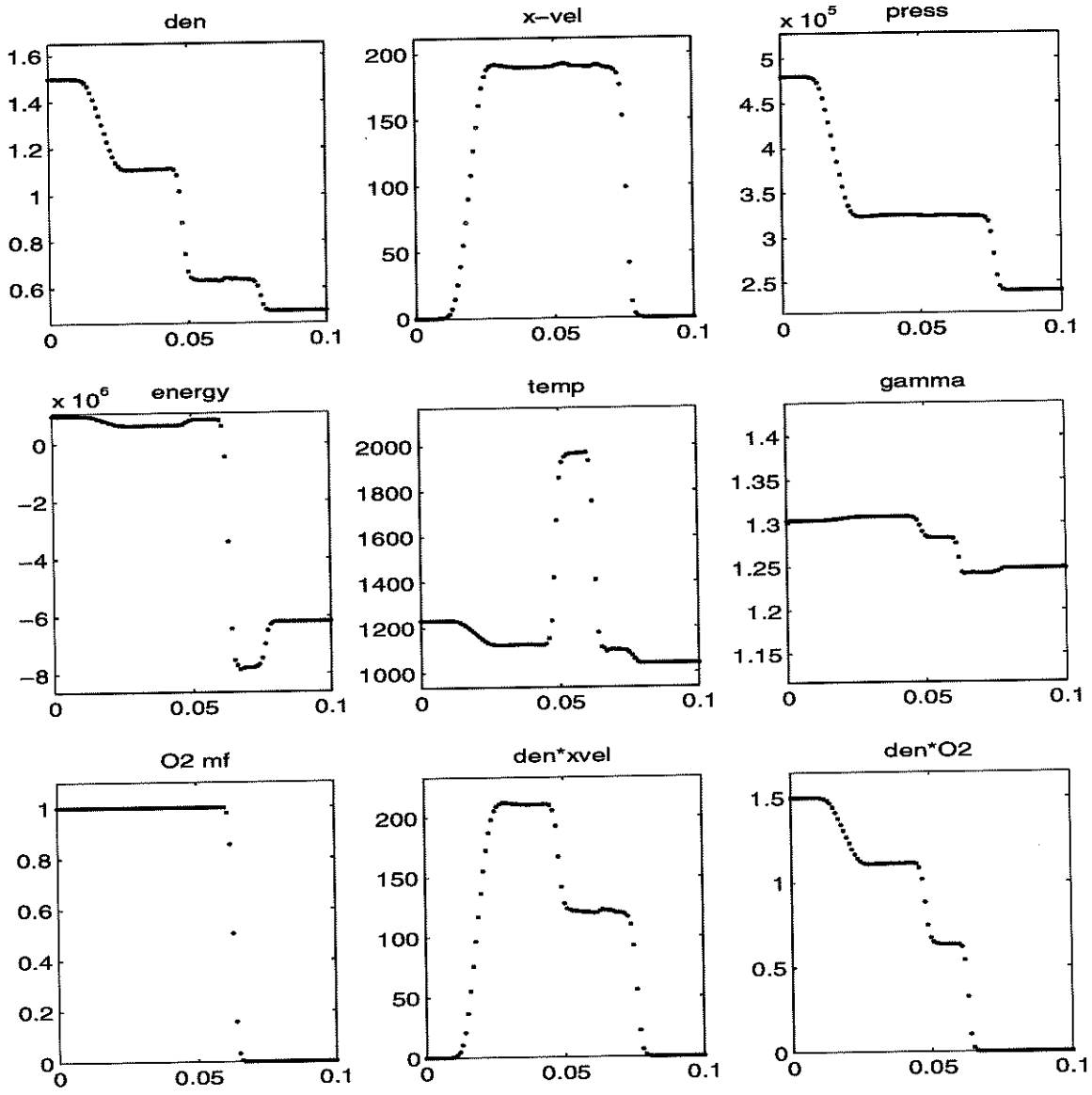

Figure 21: Example 6 - nonconservative correction - after collision - 100 points

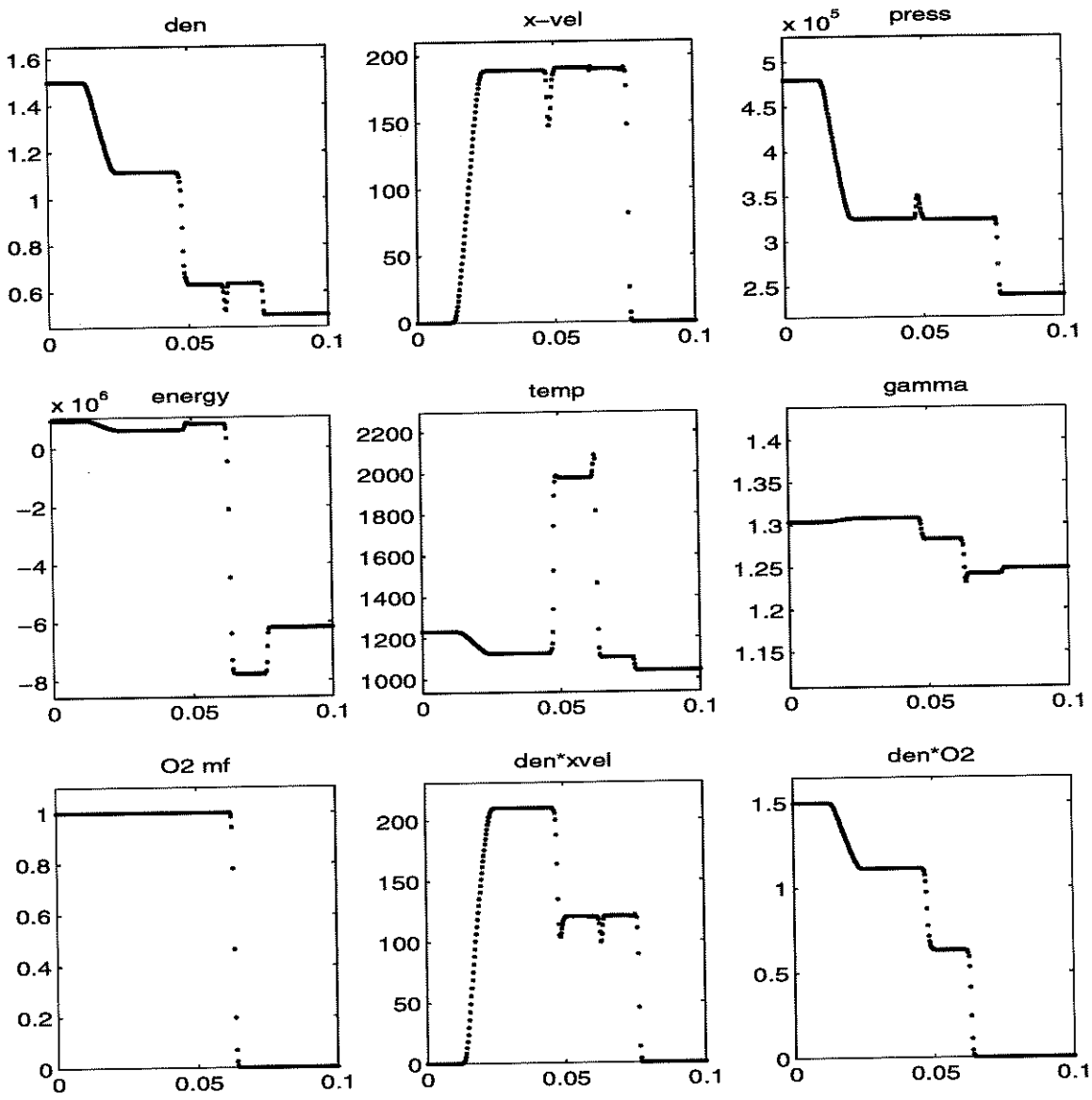

Figure 22: Example 6 - conservative method - after collision - 400 points

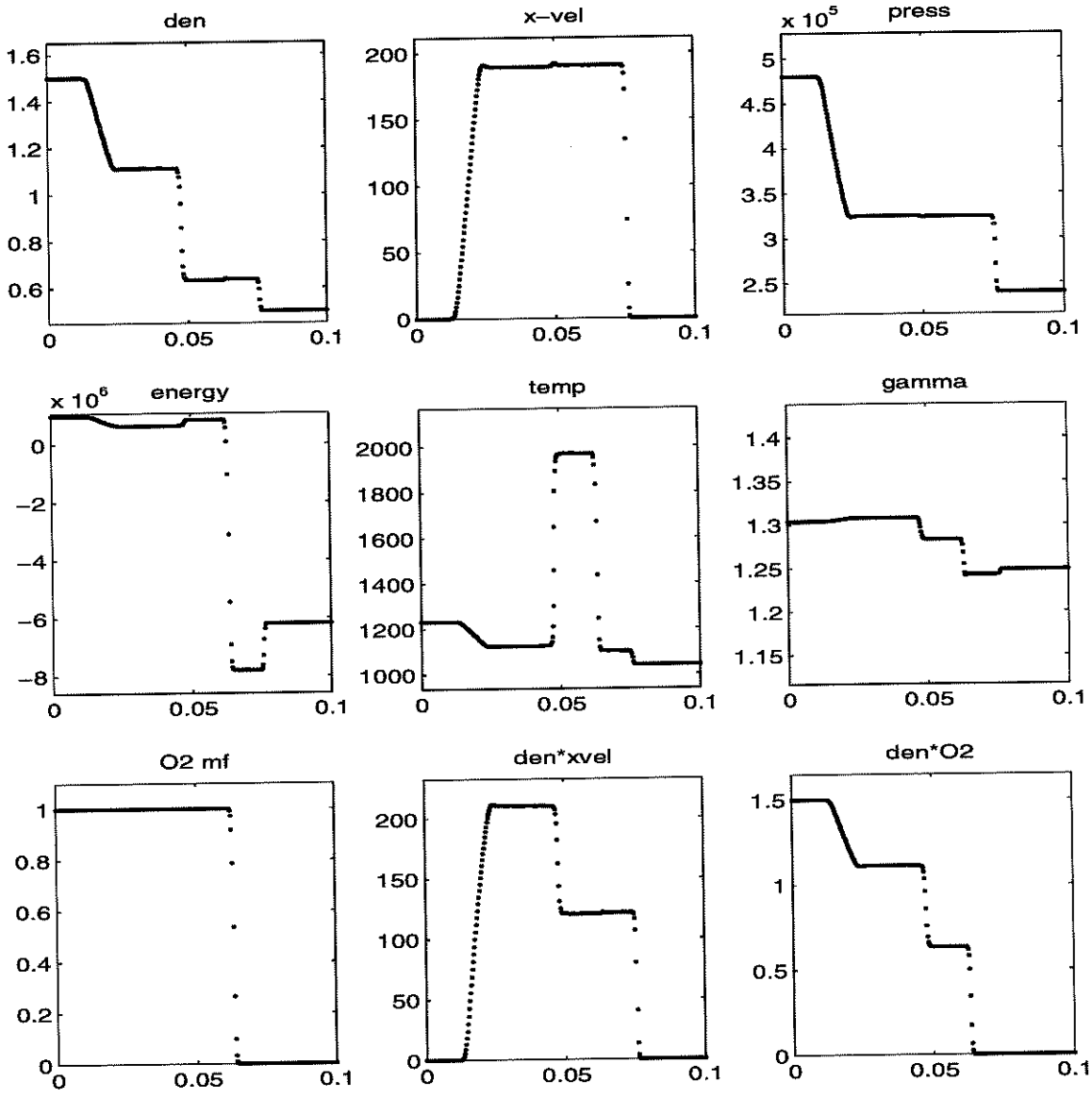

Figure 23: Example 6 - nonconservative correction - after collision - 400 points

References

[1] Fedkiw, R., Merriman, B., and Osher, S., *Efficient characteristic projection in upwind difference schemes for hyperbolic systems*, UCLA CAM Report 97-17, April 1997, http://www.math.ucla.edu/applied/cam/.

[2] Fedkiw, R., Merriman, B., and Osher, S., *High accuracy numerical methods for thermally perfect gas flows with chemistry*, J. Computational Physics 132, 175-190 (1997).

[3] Fedkiw, R., Merriman, B., Donat, R., and Osher, S., *The Penultimate Scheme for Systems of Conservation Laws: Finite Difference ENO with Marquina's Flux Splitting*, UCLA CAM Report 96-18, July 1996, http://www.math.ucla.edu/applied/cam/.

[4] Jenny, P., Muller, P. and Thomann, H., *Correction of conservative Euler solvers for gas mixtures*, Journal of Computational Physics, vol. 132, (1997), pp. 91-107.

[5] Karni, S., *Hybrid multifluid algorithms*, SIAM J. Sci. Statist. Comput. 17 (5), 1019 (1996).

[6] Karni, S., *Viscous shock profiles and primitive formulations*, SIAM J. Numer. Anal., 29 (1992), pp. 1592-1609.

[7] W. Mulder, S. Osher, and J. A. Sethian, *Computing Interface Motion in Compressible Gas Dynamics*, J. Comput. Phys., v. 100, 209-228 (1992).

[8] Quirk, J.J. and Karni, S., *On the dynamics of a shock-bubble interaction*, J. Fluid Mech. 318, 129 (1996).

[9] Sussman, M., Smereka, P. and Osher, S., *A level set approach for computing solutions to incompressible two-phase flow*, J. Comput. Phys., v. 114, (1994), pp. 146-154.